Space Programs Summary No. 37-27, Volume VI

for the period March 1, 1964 to April 30, 1964

Space Exploration Programs and Space Sciences

jpl

JET PROPULSION LABORATORY
CALIFORNIA INSTITUTE OF TECHNOLOGY
PASADENA, CALIFORNIA

May 31, 1964

Space Programs Summary No. 37-27, Volume VI

for the period March 1, 1964 to April 30, 1964

Space Exploration Programs and Space Sciences

JET PROPULSION LABORATORY
CALIFORNIA INSTITUTE OF TECHNOLOGY
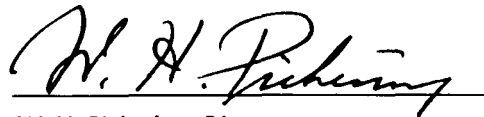PASADENA, CALIFORNIA

May 31, 1964

Preface

The *Space Programs Summary* is a six volume, bimonthly publication designed to report on JPL space exploration programs, and related supporting research and advanced development projects. The subtitles of all volumes of the *Space Programs Summary* are:

Vol. I. The Lunar Program (Confidential)

Vol. II. The Planetary–Interplanetary Program (Confidential)

Vol. III. The Deep Space Network (Unclassified)

Vol. IV. Supporting Research and Advanced Development (Unclassified)

Vol. V. Supporting Research and Advanced Development (Confidential)

Vol. VI. Space Exploration Programs and Space Sciences (Unclassified)

The *Space Programs Summary*, Volume VI consists of an unclassified digest of appropriate material from Volumes I, II, and III and a reprint of the space science instrumentation studies of Volumes I and II. This instrumentation work is conducted by the JPL Space Sciences Division and also by individuals of various colleges, universities, and other organizations. All such projects are supported by the Laboratory and are concerned with the development of instruments for use in the NASA space flight programs.

Beginning with the *Space Programs Summary 37-27* series, the Space Flight Operations Facility development progress, previously reported in Volume VI, will be reported in Volume III. The scope of Volume III is being expanded to incorporate the activities of the Deep Space Network.

W. H. Pickering, *Director*
Jet Propulsion Laboratory

Space Programs Summary No. 37-27, Volume VI

Contents

LUNAR PROGRAM

PLANETARY–INTERPLANETARY PROGRAM

THE DEEP SPACE NETWORK

SPACE SCIENCES

LUNAR PROGRAM

I. *Ranger* Project

A. Introduction

The *Ranger* Project was established to develop a space flight technology for transporting engineering and scientific instruments to the Moon and planets. Nine *Ranger* launchings, using *Atlas D–Agena B* vehicles, are now planned; six of these flights have been made.

Rangers 1 and 2 (Block I) were not lunar-oriented, but were engineering evaluation flights to test the basic systems to be employed in later lunar and planetary missions. Several scientific experiments were carried on a non-interference basis. Indications are that both spacecraft performed satisfactorily within the constraints of the obtained satellite orbit. *Rangers 3, 4, and 5* (Block II) carried a gamma-ray instrument, a TV camera, and a rough-landing seismometer capsule; all three of these flights experienced failures.

The objective of the *Ranger* Block III (*Rangers 6 through 9*) flights is to obtain TV pictures of the lunar surface which will be of benefit to both the scientific

program and the U.S. manned lunar flight program. The *Ranger 6* spacecraft, which was launched from Cape Kennedy, Florida, on January 30, 1964, and impacted the Moon on target on February 2, 1964, did not accomplish the primary flight objective due to a failure of the TV subsystem to transmit pictures. An extensive failure analysis was conducted. A document was prepared which covered the findings of the analysis as well as the recommendations for the *Ranger 7* through 9 configuration.

The *Ranger 7* spacecraft was shipped to Cape Kennedy on January 29; however, as a result of the *Ranger 6* investigation, the TV subsystem was returned to RCA and the spacecraft bus to JPL. Assembly of the *Ranger 8* spacecraft was complete and system tests had been performed; assembly of *Ranger 9* had been under way. The *Ranger 8* TV subsystem was returned to RCA. Assembly of *Rangers 8 and 9* have been rescheduled.

There has been an intensive effort to implement the modifications indicated by the *Ranger 6* failure review. RCA has been working on the redesign, rework, testing,

and integration of the TV subsystem for both the proof test model (PTM) and *Ranger 7*. A JPL task team took up residence at RCA to monitor the design, and the implementation and testing of the preventive measures taken to preclude what are believed to be the most probable causes of the *Ranger 6* failure. Another team at JPL undertook a detailed review of the remaining areas of the TV subsystem.

Modifications to the spacecraft bus were very minor and were accomplished without difficulty. The PTM TV subsystem was modified, tested, and shipped to JPL for assembly with the PTM bus. An extensive testing program is continuing. The *Ranger 7* TV subsystem was modified and tested at RCA; a comprehensive assessment of acceptability for shipment to JPL is under way.

Ranger Block IV, planned as a series of three flights, and *Ranger* Block V, planned as a six-flight series, were cancelled due to budgetary reasons by the Office of Space Sciences, NASA, in July and December, 1963, respectively.

B. Design Integration

Block III design changes since evaluation of the *Ranger 6* flight have been restricted to those that will provide a significant improvement in reliability.

The basic bus will remain the same as the *Ranger 6* bus. The most significant changes will be those which affect the interface with the TV subsystem: (1) rewiring the hydraulic timer to provide a TV enable function at separation + 30 min, (2) rewiring the solar panel actuation microswitch to provide redundant enabling to the TV subsystem, and (3) modifying the spacecraft wiring to be compatible with the new TV enabling functions. Further separation between the two sides of the TV subsystem will be provided by rewiring the Real-Time Command 7 (TV subsystem warm up) relay.

A thermal control shield has been added to reduce the temperature of the Earth sensor. The midcourse-motor chamber temperature transducer will be removed. The transducer performs no flight function, is monitored only during the midcourse portion of the mission, and breakdown (which occurred during the *Ranger 6* flight)

can cause invalidation of eight other temperature measurements.

The Sun-reacquire backup function (Real-Time Command 8) was modified to provide the central computer and sequencer with reset capability such that a midcourse maneuver can be re-initiated after being inhibited by Real-Time Command 8.

Wiring changes in the launch and system test complexes are being incorporated to provide the proper interface for the TV subsystem. As a safeguard to the spacecraft during testing, isolation resistors have been added in the operational-support-equipment power monitor J-box.

C. Systems Testing

1. Proof Test Model

After the *Ranger 6* mission, special tests were performed on the proof test model (PTM) in an effort to answer questions resulting from the mission analysis. The TV subsystem was sent to RCA for rework. The bus was disassembled, inspected, and modified in order to bring it as near as possible to the Block III configuration and to produce a spacecraft which can successfully pass the planned environmental tests. The reworked PTM TV subsystem arrived from RCA. Post-shipment checks showed the subsystem to be in good condition. TV telemetry calibrations were performed, and the TV subsystem and bus were mated.

The attitude-control gas subsystem leak test was performed. The leak rate for the subsystem was evaluated at 60 ± 10 cm³/hr. A system test and vibration tests (Fig. 1) were performed. The following problems occurred during these tests: (1) a capacitor failure in the power sync module, (2) a Sun sensor failure and a gyro saturation problem during the z-axis shake, and (3) an out-of-tolerance indication in the three-phase inverter power monitor during the lower-noise-level z-axis test. These problems are under investigation.

A series of compatibility tests between the power and user subsystems was conducted to determine peak power requirements as a function of all operational modes.
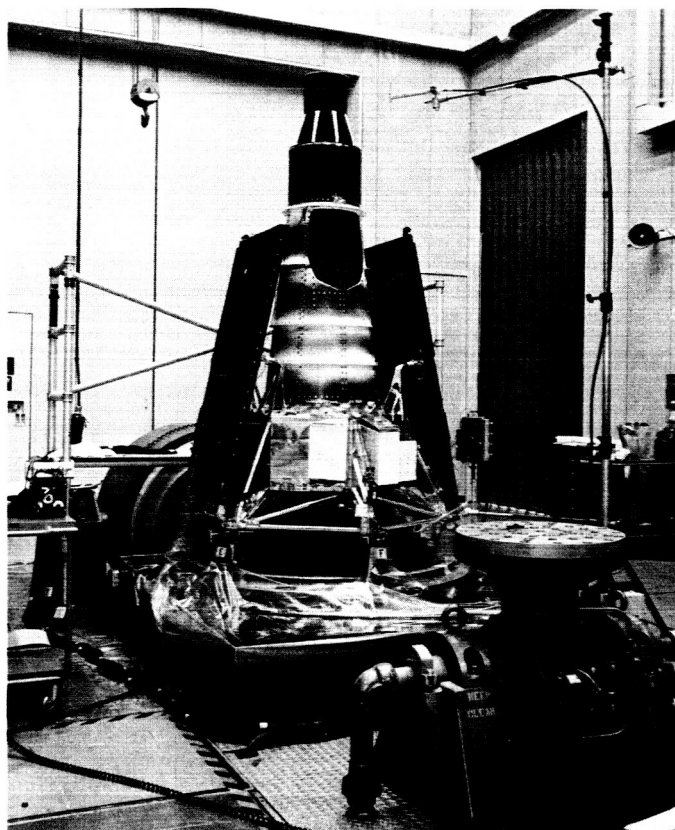
Fig. 1. Configuration for y-axis vibration of the PTM

This type of information is not normally obtainable in a spacecraft system test configuration; however, comparatively accurate readings are obtainable under laboratory conditions. The area of margin testing is also being explored. Voltages to the units are varied beyond normal ranges to establish absolute operational limits. To date, results have been very satisfactory.

2. Ranger 7

The *Ranger 7* TV subsystem was sent to RCA for rework. The *Ranger 7* bus was shipped from the Atlantic Missile Range to JPL. Changes in the flight hardware and rework on the *Ranger 7* bus consisted of the following:

(1) Both attitude-control nitrogen-gas subsystems were replaced because of contamination and leak-rate problems.

(2) A capacitor was added and a diode was removed in the central computer and sequencer to enable a maneuver to be rerun in the event of a Real-Time Command 8 maneuver inhibit.

(3) Both solar panels were replaced because hinges had been damaged.

(4) The ring harness and backup command timer were reworked because of TV modifications.

A flight pressure leak test was conducted on the attitude-control gas subsystem. Preliminary results indicated a leak rate well within specification.

All changes were checked out in subsystem tests, and a system test was performed without the TV subsystem. There were no spacecraft problems during the test.

3. Ranger 8

The electronic assemblies were removed from the *Ranger 8* bus and reworked. The filter assemblies for the attitude-control nitrogen-gas subsystems were replaced. A spring constant determination provided additional information on the previously reported spring constant test. Preliminary evaluation of the data indicated that the problem (the spring constant was too soft) was with the flight adapter.

The *Ranger 8* TV subsystem and all TV spares were returned to RCA for rework. All operations on the *Ranger 8* bus have been suspended until the latter part of 1964.

D. Inflight Performance of the *Ranger 6* Attitude-Control Subsystem

1. System Description

The attitude-control subsystem is designed to control the orientation of the spacecraft with respect to the Sun and Earth and to point the high-gain antenna toward Earth. Angular orientation errors with respect to the reference bodies are sensed by optical Sun sensors and an Earth sensor. Separate Sun sensors control the pitch and yaw axes; the Earth sensor controls the roll axis and the hinge orientation of the high-gain antenna. Subsystem damping is provided by rate signals from three single-axis floated gyroscopes with torque rebalance loops.

Control torques about the spacecraft axes are produced by a cold nitrogen gas expulsion subsystem. This subsystem utilizes four gas expulsion jets per axis, two for the clockwise direction and two for the counterclockwise direction, for a subsystem total of twelve jets. Gas flow through individual jets is controlled by solenoid valves. Each solenoid valve pair is operated by a signal from a switching amplifier having a bistable output switch. The switching amplifier inputs are the rate and position signals for the respective vehicle axes. When the sum of the rate and position signals exceeds a predetermined value, or "deadband," the amplifier actuates the pair of solenoid valves that will produce a torque opposing the direction of the rate-plus-position error. A controlled hysteresis in the bistable output switches prevents the valves from turning off until the error signal reaches a prescribed level below the turn-on level. This hysteresis establishes a minimum impulse that is imparted to the vehicle on each valve actuation and thus prevents possible valve chatter.

Reorientation of the spacecraft for the midcourse velocity correction is accomplished by a roll–pitch turn sequence in response to commands from the central computer and sequencer. This command disables the Sun and Earth sensors and connects a command current generator to the respective gyro torquer; the gyro senses the difference between the command rate and the actual vehicle rate. Position error is obtained by inserting an integrating capacitor in the gyro rebalance loop. When the turn command is removed, the gyro retains the position reference.

A midcourse autopilot maintains the spacecraft orientation during the midcourse motor firing. Vehicle rate and position are sensed by the gyros, and control torques are produced by jet vane control of the midcourse-motor thrust.

2. Inflight Performance

The inflight performance of the *Ranger 6* attitude-control subsystem was normal in all respects and is summarized below.

Acquisition. Upon receipt of the Sun-acquisition command, the vehicle tumbling rates were 5.0, −9.6, and 2.6 mrad/sec in pitch, yaw, and roll, respectively. The spacecraft acquired in pitch and yaw within 4 min after receipt of the acquisition command. The roll rate was reduced to 0.9 mrad/sec within 10 sec.

Upon receipt of the Earth-acquisition command, the vehicle accelerated to a roll search rate of −3.8 mrad/sec.

After a 20-min, 40-sec roll search, the Earth sensor detected Earth light, and it completed the acquisition 25 min after receipt of the command. It is estimated that the spacecraft rolled through a 270-deg angle in the roll search.

Cruise. The attitude-control subsystem stabilized the spacecraft position within the nominal ±2.8-mrad deadband in pitch and yaw. Roll position stabilization was within the normal deadband limits, which vary with the distance from Earth. The limit cycle velocity increment was within the design maximum of 90 μrad/sec. An external pitch torque of −170 dyne-cm was determined from the limit cycle data. No steady external torques were evident from the roll and yaw data.

Midcourse maneuver. The midcourse maneuver required for the trajectory correction consisted of a 54-sec negative polarity roll turn and a 328-sec negative polarity pitch turn. The limit cycle positions at the start of the roll turn were: roll, 2.8 mrad; and pitch, 0.0 mrad. Both turns were executed in a normal manner, and the rate transients compared well with the expected values. The predominant source of error in the midcourse maneuver is the initial roll limit cycle position. Since this initial condition was small compared to its maximum predicted value of 8.8 mrad, a very small midcourse pointing error resulted.

The autopilot transients compared well with predicted values from an analog computer study.

Reacquisition. Upon receipt of the Sun-reacquisition command, the spacecraft accelerated to a pitch rate of 4.9 mrad/sec and reacquired the Sun in 5 min. The yaw rate and position remained at null during the reacquisition.

At the end of the midcourse-motor burn, the residual roll rate was 100 μrad/sec. This rate reduced the roll position error relative to the Earth from 11.4 deg (introduced by the midcourse roll turn) to approximately −1 deg at the time of Earth reacquisition. The Earth sensor detected the Earth as soon as it was turned on, and the acquisition was completed within 80 sec.

Antenna hinge control. The hinge subsystem tracked the Earth within the 1.25-deg deadband of the hinge angle servo during cruise operation. During Sun acquisition the antenna was extended to the preset angle of 135 deg inserted before launch. During the midcourse maneuver sequence, the antenna moved in a normal manner to the 180-deg exit angle and then to the 122-deg reacquire angle at Sun reacquisition.

Gas subsystem. The control acceleration of the gas subsystem was within the specification range of 0.54 to 0.66 mrad/sec². Based on the observed 60- to 90-μrad/sec velocity increment, the gas consumption is estimated to be 0.1 to 0.4 lb, which is insignificant compared to the 1.15-lb calculated worst-case value. No measurement of the actual consumption is possible due to the 0.08-lb accuracy of the telemetered measurements and the uncertainty of the gas reservoir temperatures.

Earth sensor. The measured Earth brightness was consistently 2 to 4 times the expected value. This is accounted for by the difference in color temperature between the calibration source and the Earth and by the accuracy of the calibration meters. There is also an uncertainty in the predicted Earth brightness because of variation of the Earth's albedo.

E. Postflight Analysis of *Ranger 6* Midcourse Propulsion Subsystem

The propulsion subsystem parameters telemetered to Earth during the firing of the midcourse propulsion subsystem include: (1) the high-pressure nitrogen reservoir pressure, (2) the fuel tank pressure, (3) the nitrogen tank temperature, (4) the hydrazine reaction chamber wall temperature, and (5) the fuel tank temperature. The first four parameters were available at a high sampling rate of from 6 to 300 readings/min, whereas the last parameter was scanned once every 1000 sec (16⅔ min).

Shortly after the ignition of the propulsion subsystem during the *Ranger 6* midcourse maneuver, the reaction chamber wall temperature transducer underwent a shift and shorted when the chamber reached steady-state temperature. The temperature–time history until the shift occurred indicated that a normal ignition had been obtained. The nitrogen tank temperature and chamber
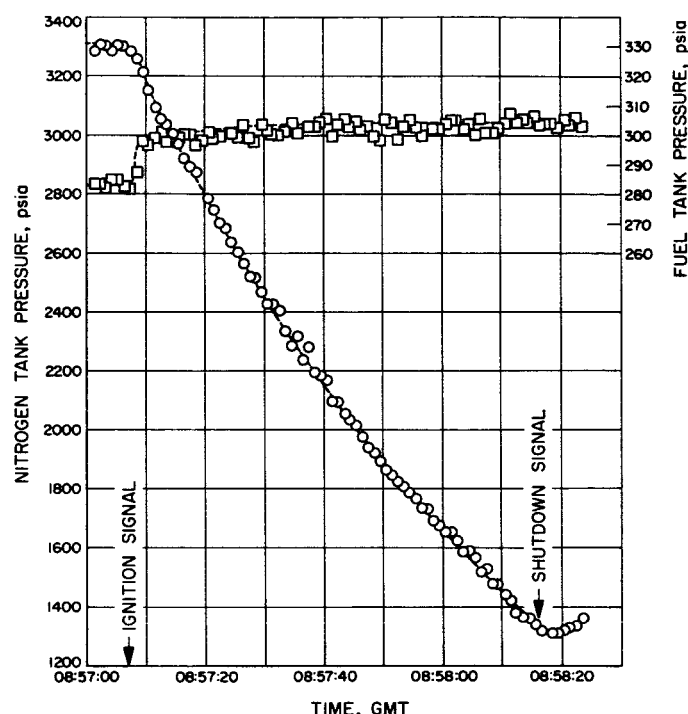

Fig. 2. Variation of propulsion system pressures during motor-burn period of midcourse maneuver

temperature measurements utilize the same reference circuitry in the telemetry system. Thus, the loss of the chamber temperature transducer caused the invalidation of the nitrogen tank temperature measurement, since the reference bridge had been severely unbalanced.

Therefore, only two pressure measurements (high-pressure nitrogen reservoir and fuel tank) were available during most of the motor-burn period. The variation of these two parameters during this period is illustrated in Fig. 2. The fuel tank pressure undergoes an abrupt change at ignition since high-pressure nitrogen gas is released to the pressure regulator at this time. Regulated pressure is normally very stable; the scattered data points are believed to be caused by instrumentation noise which is typical of the high-sampling-rate parameters. The nitrogen tank pressure decay curve is typical of such a process, with limited heat transfer occurring between the gas and its surroundings during the blow-down process.

II. *Surveyor* Project

A. Introduction

The *Surveyor* Project will take the next step in advancing lunar technology by making soft landings on the Moon, beginning in 1965 with a group of four test missions whose objective is to demonstrate successful soft landing by post-landing spacecraft operation. An engineering payload including elements of redundancy, increased diagnostic telemetry, touchdown instrumentation, and survey TV will be used.

The general objective after 1965 is to perform operations on the Moon contributing new scientific knowledge and basic data in support of manned lunar landings. A group of four flights planned for 1966 will carry a scientific payload selected from the following experiments: two-camera TV, micrometeorite ejecta, single-axis seismometer, alpha-particle scattering, soil properties (surface sampler), and touchdown dynamics.

In 1965 and 1966, the 2150-lb (separated weight) spacecraft will be injected into the lunar trajectory by direct ascent, using single-burn *Atlas–Centaur* vehicles.

In a preliminary study, it was concluded that the *Surveyor* spacecraft payload can be increased significantly by using 90-hr transfer trajectories instead of the currently planned 66-hr transfer trajectories. A detailed study is being initiated to rigorously determine the feasibility and desirability of 90-hr transfer trajectories for the *Surveyor* mission.

Hughes Aircraft Company is under contract to develop and manufacture the first seven spacecraft.

B. Space Flight Operations

Functional requirements were established for two computer programs which will process spacecraft data at the Deep Space Instrumentation Facility sites and provide spacecraft simulated data to be used extensively during future testing of the space flight operations system.

The Deep Space Network proposal for the mission-independent on-site computer configuration was extended to include all *Surveyor* mission-dependent requirements. Implementation of the over-all on-site data-processing system design is proceeding. Communication line usage under various operational conditions has been established, and spacecraft data alarm monitoring techniques have been defined.

C. Spacecraft System Development

The following material relating to the *Surveyor* spacecraft system development was prepared by the Hughes Aircraft Company. The principal model designations and vehicles discussed are defined in Table 1.

Table 1. Model and vehicle designations

Designation	Description
SC-1–4	Flight spacecraft with engineering payload
SC-5–7	Flight spacecraft with scientific payload
A-21	Model designation for spacecraft with engineering payload (SC-1–4)
A-21A	Model designation for spacecraft with scientific payload (SC-5–7)
T-21	Model A-21 prototype system test spacecraft
T-21A	Model A-21A prototype system test spacecraft
T-2	Simplified spacecraft for evaluation of terminal descent propulsion and flight control
S-2	Test spaceframe for vibration, shock, and static structural tests
S-6, -7	Test spaceframe for vernier propulsion system tests
S-8	Test spacecraft for flight control buzz tests

System engineering. A three-volume functional description of the A-21 spacecraft has been completed. The SD-4 type approval model of the *Surveyor* dynamic vehicle for use in *Centaur* tests successfully completed testing and was shipped to Lewis Research Center in February 1964.

Scientific payload. The engineering change proposals for incorporation of scientific instruments in the A-21A spacecraft were approved by JPL, and spacecraft/instrument interface specifications were revised accordingly. Instrument test plans and equipment are being re-evaluated. As a result of experience with the survey

camera in T-21 system testing, changes are being made to prevent oscillations in the mirror drive circuit and undesirable interactions among the camera, transmitter, and central command decoder. The variable-focal-length lens design was modified to prevent a shift-of-focus and decentration problem.

System analysis. Study of earlier switching of the transmitter to the high power mode to provide added telemetry prior to *Centaur* separation indicated that high-power operation cannot be started prior to shroud ejection; the restraints due to the resulting temperature rise in Compartment A were evaluated. The program for postlanding spacecraft attitude determination was formulated. A computer routine has been designed for generating simulated spacecraft telemetry data for use in system checkout.

Flight control. In structural coupling tests with the S-2 vehicle, no inertial control loop instability was encountered under simulated vernier engine vibration inputs. Acceptance tests were completed on the first flight models of the secondary Sun sensor, inertial reference unit, and electronics unit. Type approval testing of the gas jet valves and the inertial reference unit was completed.

Electronics. Coverage of the single omnidirectional antenna as mounted on the spacecraft dynamic test vehicles was measured with a full-scale model. Steps are being taken to prevent excessive heating and cooling of the altitude marking radar under mission conditions. Investigation of vibration problems encountered in type approval tests of the radar altimeter and doppler velocity sensor is continuing; an improvement was made in the klystron to meet the 250-hr life requirement. Circuit improvements were made in the electrical converter unit for the central command decoder in order to reduce waveform spikes in the switching transistors and various outputs.

Electrical power supply. Type approval testing of the solar panel was successfully completed, and flight acceptance testing of the first flight panel has begun. A statistical analysis of performance at Table Mountain, California, indicates that the solar panel output meets requirements. Structurally improved battery cells were vibration tested with satisfactory results, and main batteries incorporating the changes are scheduled for testing in early May. Three auxiliary batteries passed type approval tests.

Thermal control. An overall design review of thermal control provisions was held on March 31. Compartment design changes resulting from S-2 vibration test experience were evaluated with respect to thermal control.

Thermal design requirements for the alternate vernier thrust chamber assemblies were studied. Thermal provisions for simulated lunar day and night testing of the T-21 spacecraft have been defined.

Engineering mechanics. In the touchdown dynamics program, data from the S-2 drop tests are being used to upgrade the rigid-body mathematical model; the improved model will increase the accuracy of the elastic-vehicle computer program. Modifications were incorporated in the landing gear shock absorber due to the failure of a developmental model in drop tests; two type approval units exhibited satisfactory strength in further drop tests. Two structural failures occurred in drop testing of the S-2 vehicle; the vehicle, presently being upgraded to incorporate structural improvements and to represent the current spacecraft configuration, will be retested.

Propulsion. The main retro-engines were successfully fired with the thermal gradients expected in a mission. Burst tests of two engine cases confirmed satisfactory design margins. The retro-engine design was frozen, and qualification tests will be conducted in July. Development of the vernier thrust chamber at the Thiokol Chemical Corporation, Reaction Motors Division, was terminated, and an evaluation of alternate thrust chamber assemblies was completed. A tank development program, including welding processes for aluminum tanks and manufacture of titanium tanks, is under way. The S-7 vernier propulsion test vehicle completed vibration tests and was shipped to the Air Force Missile Development Center (AFMDC) for further tests involving the use of propellants.

Spacecraft vehicle and mechanisms for basic bus. A new spacecraft for T-21A is being built to replace the one reassigned to the S-8 buzz test vehicle; A-21A substructure design work has started in accordance with the recent decisions on the scientific payload. S-8 substructure fabrication has begun, and preparations have been made to reinforce the Aerobee tower for the buzz tests. The lightweight landing gear successfully completed the dynamic portion of type approval tests. Two structural improvements in the omnidirectional Antenna A mechanism are being made as a result of hardware failures in type approval tests. Increased strength is also being built into the antenna/solar panel positioner so that it will be able to withstand the loads encountered in vibration tests of the S-2 vehicle.

Reliability, quality assurance, and system test. Reliability estimates were upgraded, and vendor surveillance was maintained continuously. Reliability margin testing of pyrotechnic devices is under way. Various thermal coatings and repair procedures were evaluated. Quality assurance activities included improvement in documentation of standard fabrication practices, implementation of quality audits in all Hughes work areas, and continuing audit of subcontractor effort. Two additional series of T-2 horizontal static firing tests were completed to evaluate acoustic shields on the radar antennas and radar reaction with the spacecraft footpads; descent dynamics tests of the T-2 vehicle in drops from a tethered balloon will begin during the next report period. The first pass through type approval functional testing of the T-21 spacecraft (except for vernier propulsion, television, and telecommunications systems) is nearly complete, and the spacecraft will be upgraded early in the next report period. A high-frequency vibration test on T-21, with inputs at the vernier engine brackets, was made to obtain realistic vibration test parameters for the radar altimeter and doppler velocity sensor (RADVS) system.

Mission operations. Procedures were formulated for the spacecraft readiness tests to be performed at the launch complex prior to removal of the gantry from the launch vehicle. The overall launch complex operations were described in the Launch Complex Operations Directive released during this report period. Operation of the programmed automatic telemetry evaluator in conjunction with the command and data handling console (CDC) was demonstrated. The Launch Operations Plan, the primary document for coordination of all operations and tests required for a *Surveyor* launch, was released. The CDC for the Goldstone Tracking Station was shipped on April 9.

Study on Block II Surveyor. A study was completed on the Block II *Surveyor*, proposed for soft landing lunar payloads in the period from 1967 to 1969. Minimum change from the A-21/A-21A (Block I) basic bus was assumed. Payload capability was determined for various combinations of alternatives, including spacecraft injected weight, vernier propulsion throttle range, main retro case material and propellant type, and transit trajectory class. Payload weights varied from 157 to 318 lb in the 18 configurations compared in this study. Use of a radioisotope thermoelectric generator in the power system and an increase in landing area and accuracy were also considered.

THE PLANETARY – INTERPLANETARY PROGRAM

III. *Mariner* Project

A. Introduction

The early objective of the Planetary-Interplanetary Program is the initial probing of the planets Mars and Venus by unmanned spacecraft. The initial probing of Venus was successfully accomplished by *Mariner 2*. The next step toward this objective is the initial probing of Mars by a *Mariner C* spacecraft planned for the 1964–1965 opportunity.

The primary objective of the *Mariner C* mission (*Mariner* Mars 1964 Project) is to conduct closeup (flyby) scientific observations of the planet Mars during the 1964–1965 opportunity and to transmit the results of these observations back to Earth. The planetary observations should, to the greatest practical extent, provide maximum information about Mars. A TV system and a reasonable complement of field and particle experiments will be carried.

A secondary objective is to provide experience and knowledge about the performance of the basic engineering equipment of an attitude-stabilized flyby spacecraft during a long duration flight in space farther away from the Sun than the Earth. An additional secondary objective is to perform certain field and/or particle measurements in interplanetary space during the trip and in the vicinity of Mars.

It is planned to conduct two launchings of *Mariner C* missions from two separate pads. All activities will be planned to exploit the limited launch period to the maximum extent. To accomplish this, spacecraft and launch vehicles will be processed in parallel, so that following the launch of the first space vehicle the second vehicle may be launched without delay, no earlier than two days after the first.

The proof test model was subjected to a series of mission environment simulation tests, and although the tests were not entirely without anomalous occurrences, they were considered highly successful. These tests included a continuous 10-day mission test in the 25-ft Space Simulator, a 4-day thermal balance test in the same simulator, vibration and acoustic tests, and a mapping of the spacecraft magnetic field on a new specially designed fixture.

B. System Testing

System Test 2 was performed to test the complete proof test model spacecraft with all known deficiencies removed and with all the latest engineering change requirements incorporated. The major problem experienced during the test was an abnormal encounter sequence, which probably resulted from a supersaturated spot on the vidicon tube. Another area which might have caused the abnormal sequence could be in the TV shutter. The problem is being resolved.

Permanent field mapping was performed on the spacecraft, using a specially designed fixture (Fig. 1). Preliminary reports indicated that a 50-gamma field was measured at the sensor due to the permanent magnetic field of the spacecraft.

The thermocouples, solar panel stubs, attitude control special gas manifolds, and thermal shields were installed on the spacecraft (Fig. 2). System verification tests were performed. During the tests, difficulty was experienced in obtaining the narrow-angle Mars acquisition via the narrow-angle Mars gate by direct command. However, a normal science encounter sequence could be attained using the TV planet-in-view signal. Also, the solar vane actuators could not be driven in both directions. The effect of gravity was analyzed as the cause. Despite these problems, testing proceeded.
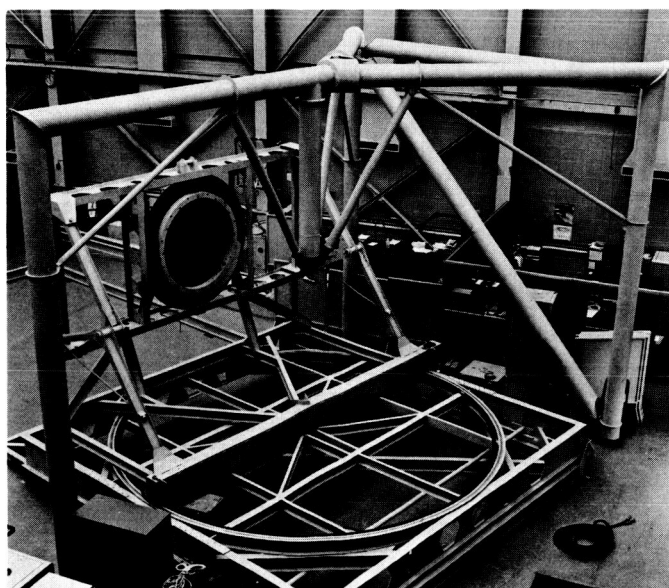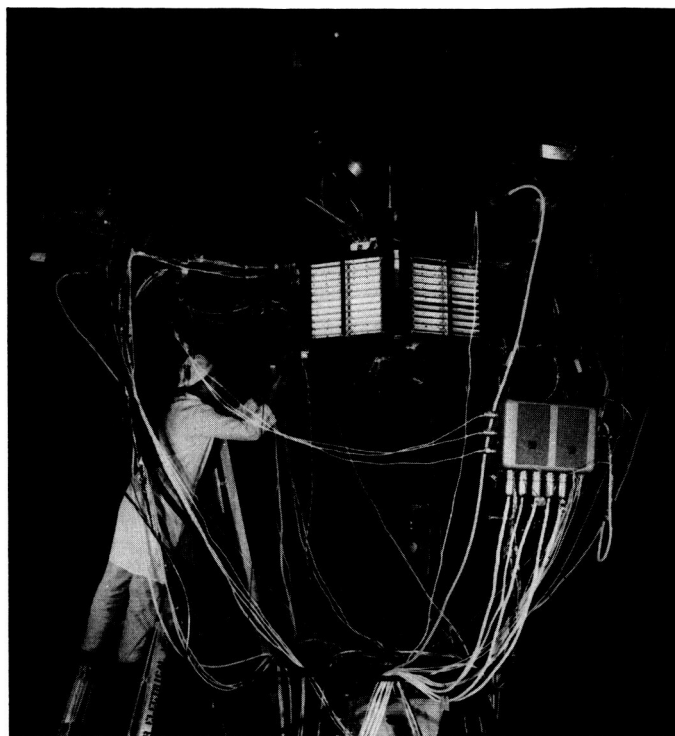

Fig. 2. **Mariner C spacecraft being prepared for the Space Simulator**

The 10-day space simulator test was performed. This test established the functional integrity of the spacecraft while operating in a simulated flight environment.

Throughout the space simulator test the radio system did not perform normally with either Power Amplifier A or B. The problem was apparently caused by a lack of a thermal path for the cavities baseplates. The central computer and sequencer (CC&S) operational support equipment caused several abnormal behaviors which resulted in incorrect times being issued for CC&S commands.

The attitude-control Sun sensor stimuli lights failed, and the only valves that could be actuated were the + yaw and roll jets. This failure was due to an improper design that did not permit the light heat to be carried off by conduction. The cosmic dust accumulators showed some spurious counts.

Despite some difficulty in the video storage subsystem area during the encounter record sequence, the test objective was not invalidated. The TV picture data was played back satisfactorily.

After the space simulator test, the spacecraft was excited in torsional and lateral axes and subjected to

Fig. 1. **Magnetic mapping fixture**

acoustic vibration. The spacecraft passed all axes of shake except that the scan cover latch mechanism tore loose and the Canopus sensor failed. Both discrepancies are being resolved.

C. Spacecraft Design and Development

1. Antenna Structures

The *Mariner C* trajectories require that the low-gain antennas provide roll-axis pattern symmetry with strong forward-hemisphere pattern coverage. The *Mariner C* low-gain antenna design (Fig. 3) meets this requirement. The design provides a 7-ft-high antenna position with line loss less than 0.01 db for a total weight of less than 4 lb. A circular waveguide electrically feeds and structurally supports the low-gain antenna, thereby eliminating coaxial weight and line losses. The antenna itself is a simple crimped termination to the waveguide. No support truss is required because the 4-in.-D tubular waveguide has a structural function. Brackets for mounting the magnetometer and ion chamber experiments are easily bonded to the outside of the tube. Structural resonances are reduced by attaching two damping struts, each with a spring and dashpot, to the waveguide.

The high-gain antenna reflector (Fig. 4) is an elliptical section of a parabolic shell fabricated from ultra-thin-gauge aluminum honeycomb. The skins of the parabolic reflector are drawn from sheets of 4-mil aluminum foil

and are bonded to an aluminum honeycomb core of ¼-in. cells with 0.7-mil walls. Lightweightness of the feed and feed support truss (fiberglass) was accomplished by proper application of minimum-gauge high-temper aluminum alloy machinings. The total weight of the 4-ft long, 21-in. wide elliptical reflector is 2 lb (or a weight distribution of 0.0025 psi of face surface) and its lowest structural resonant frequency is 120 cps.

2. Thermal Shields

The sides of the structure (electronic box faces) are covered with 0.012-in. polished aluminum shields. Some of the shields contain cutouts which allow heat to be radiated from local "hot spots." The shield designs are modular, attach to the chassis at standard locations, and therefore allow a high degree of versatility.

The upper and lower portions of the octagon, including the science platform, are shielded by multilayers of crinkled aluminized Mylar. The outer and inner layer of each blanket is covered with either black Dacron, if the shield is in the sunlight, or aluminized Teflon. The outer Teflon and Dacron layers provide the desirable thermal radiator surfaces, and the inner Teflon layers reduce the chances of the thin Mylar being torn by sharp edges.

3. Structural Dampers

The solar panel boost dampers (Fig. 5) provide damping and positioning of the solar panels during the boost phase of the mission. These dampers consist of two concentric aluminum tubes which contain a beryllium-copper spring and are filled with 500,000-cs silicone oil. Each of the two dampers is attached to the upper structure ring
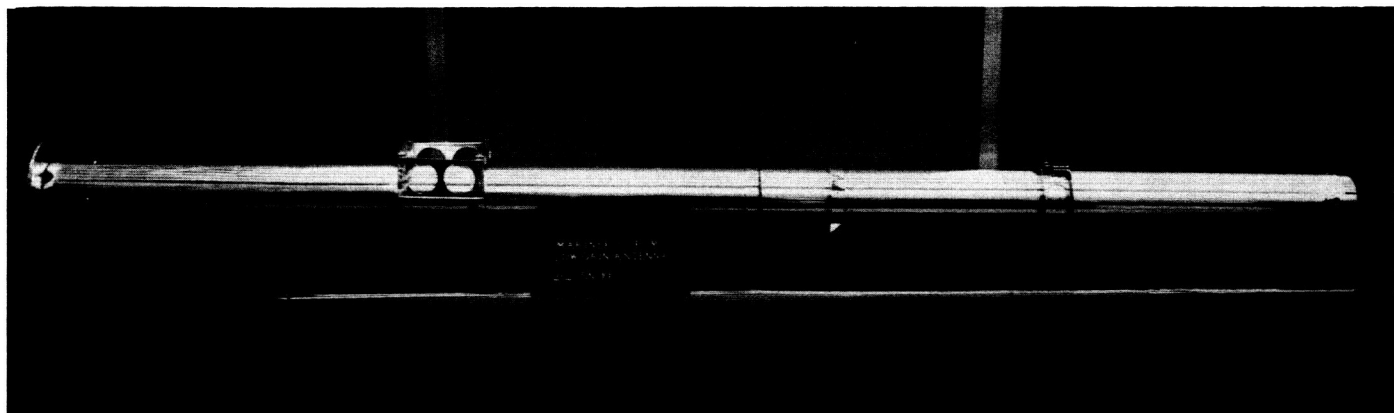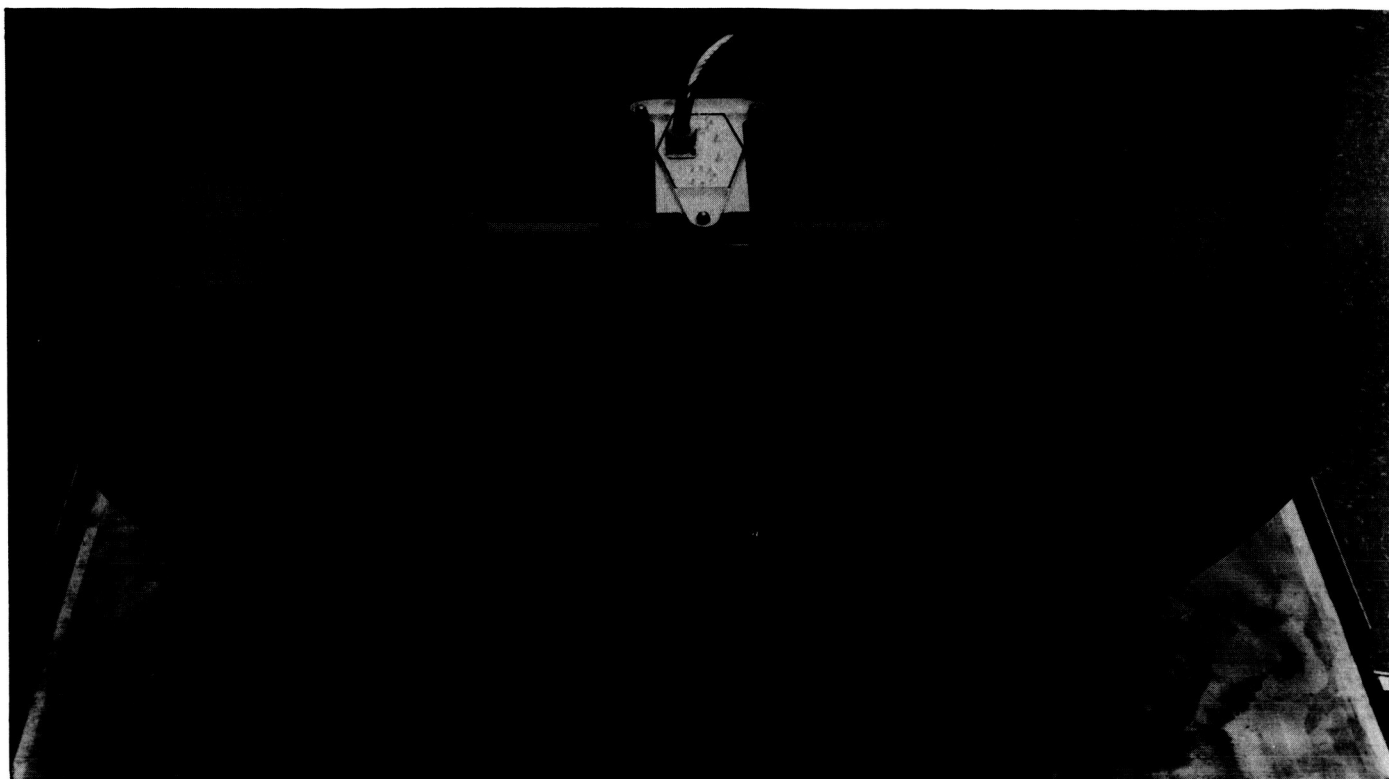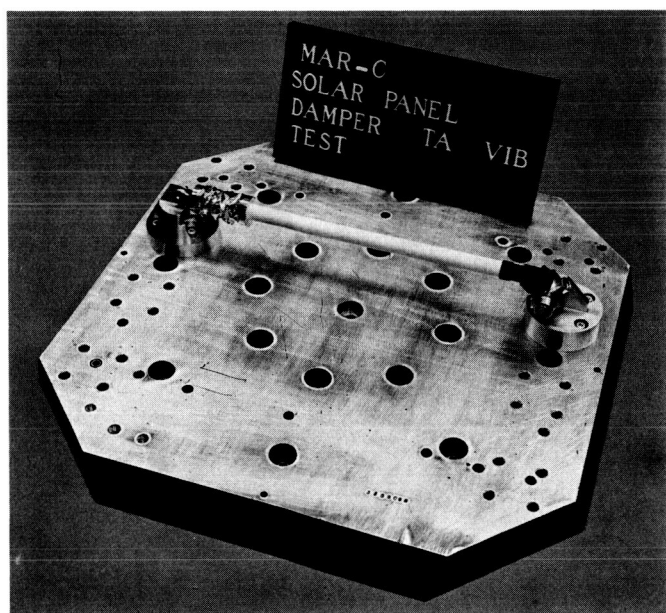

Fig. 3. Low-gain antenna

Fig. 4. High-gain antenna
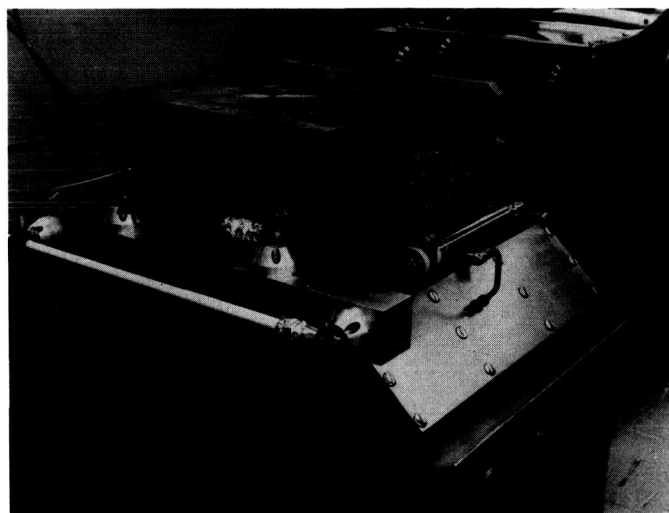

Fig. 5. Solar panel boost damper

Fig. 6. Low-gain antenna dampers

The low-gain antenna dampers (Fig. 6) are used to provide damping and positioning to the low-gain antenna during boost, and positioning throughout the mission. These dampers are basically the same as the solar panel boost dampers. Each of the two low-gain antenna dampers has different damping, spring force, and length requirements because they are not symmetrically placed

by a monoball rod end bearing, and to the solar panel by a pyrotechnic pin puller mounted to the damper. At the termination of the boost phase, the panels are released from the dampers by means of the pyrotechnics.
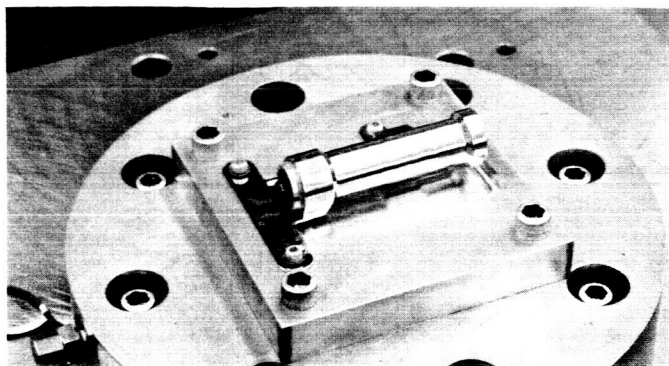
Fig. 7. Solar panel cruise damper

with respect to the spacecraft bus and the low-gain antenna.

The solar panel cruise dampers (Fig. 7) provide damping and positioning of the solar panels with respect to the spacecraft bus during the midcourse maneuver. These are conventional piston-type oil dampers utilizing a relatively low viscosity oil of 1000 cs. These dampers make use of a piston-type volumetric compensator to allow for oil expansion, and a nylon damping piston in a magnesium cylinder to provide damping force compensation

due to temperature changes. Engagement of the cruise damper latches to the solar panel is the terminal event in the panel deployment sequence.

4. Separation-Initiated Timer

The separation-initiated timer (Fig. 8) is composed of a spring-loaded, hydraulically damped plunger which initiates motion on spacecraft separation from the *Agena*. The timer provides the necessary switching sequence to allow the pyrotechnic control assembly to activate the solar panel and scan platform pinpullers. Backup functions are incorporated in the spacecraft system.

The timer type-approval unit and all flight units have been qualified with no failures. Systems compatibility tests run on the spacecraft demonstrated that the basic purpose of the timer assembly has been fulfilled.

5. Pyrotechnic Arming Switch

The pyrotechnic arming switch (Fig. 9) consists of a bank of four hermetically sealed microswitches actuated by two beryllium-copper leaf springs. The leaf springs rest on a pad on the *Agena* adapter, holding the microswitches in the open position. At separation, the leaf
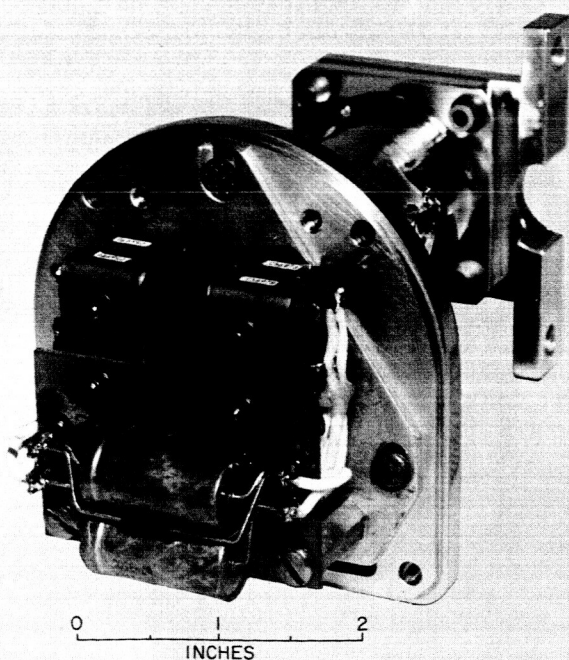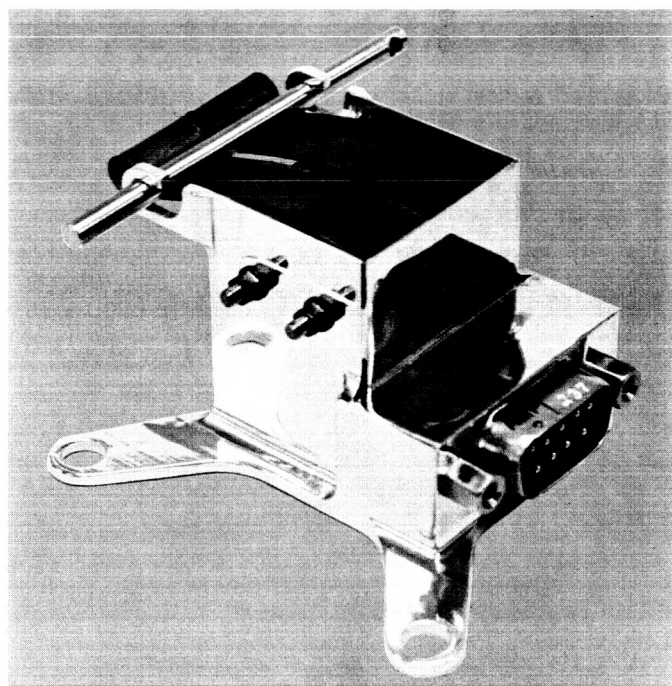

Fig. 8. Separation-initiated timer

Fig. 9. Pyrotechnic arming switch

springs are free to move, closing the circuits, and connecting the pyrotechnic control assembly and the attitude-control subsystem to power. Pyrotechnic arming is backed up by the separation-initiated timer, and attitude-control turn-on is backed up by the central computer and sequencer in the event of a pyrotechnic arming switch failure.

A pyrotechnic arming switch was subjected to type-approval and flight acceptance tests. No failures were noted.

6. Pyrotechnic Control Assembly

The pyrotechnic control assembly utilizes both silicon-controlled rectifier switches and latching relays. The assembly performs seven firing functions upon command: pin retraction of the solar panel and science platform latches; first start, first stop, second start, second stop for two midcourse motor firings; and solenoid release for the science cover.

Arming of the pyrotechnic assembly is accomplished from either the separation-initiated timer or the pyrotechnic arming switch. The latter is actuated immediately upon separation of the spacecraft from the *Agena*.

The firing unit was designed and sized to reliably fire 1-amp/1-w midcourse propulsion squibs, which require 0.03 joules per squib. Redundant squib firing is achieved through the use of two identical, interchangeable firing units along with dual squibs or dual bridgewire squibs on each pyrotechnic device.

Power and firing command inputs are not redundant except for the command to fire solar panel squibs. The latter command originates from the separation-initiated timer and the central computer and sequencer. Receipt of the command from either source will command all solar panel and science platform pinpuller squibs to be fired.

Power demand from the spacecraft is kept to a minimum by using capacitor-discharge squib-firing techniques. Two capacitor banks are required in each redundant unit to meet the minimal midcourse motor burn time. One bank fires midcourse motor on-squibs, the other fires midcourse motor off-squibs.

Midcourse motor second-burn squibs are commanded to fire through transfer latching relays within the firing units. The relays are actuated from the command sub-

system. Midcourse motor inhibit relays, within the firing units, may also be actuated from the command subsystem.

7. Solar Panels

The *Mariner C* flight solar panel is 35.5 × 71.4 in. (17.6-ft² surface area) and weighs 18.7 lb. The total weight of the four solar panels on the *Mariner C* spacecraft is 74.8 lb, excluding the deployment mechanisms and attitude-control equipment.

Solar cell temperature is expected to be 59°C after stabilization in space near Earth and is expected to decrease to approximately −12°C at Mars encounter.

The nominal power of the total array (28,224 cells) is expected to be 690 w at the maximum power voltage for cruise conditions in space near Earth. The nominal power capability decreases to approximately 299 w at Mars encounter. The nominal and maximum reliable power that can be used by the power regulator assembly is shown in Fig. 10. The maximum reliable power is approximately 81% of the nominal power.

8. Autopilot Subsystem

The *Mariner C* spacecraft has the capability of correcting its trajectory by firing a small rocket motor. The function of the autopilot is to maintain a stable and accurate vehicle attitude during the rocket-motor firing. The autopilot uses three gyroscopes to sense motion about the three spacecraft axes, and it applies corrective torques by positioning four jet vanes in the rocket exhaust stream.
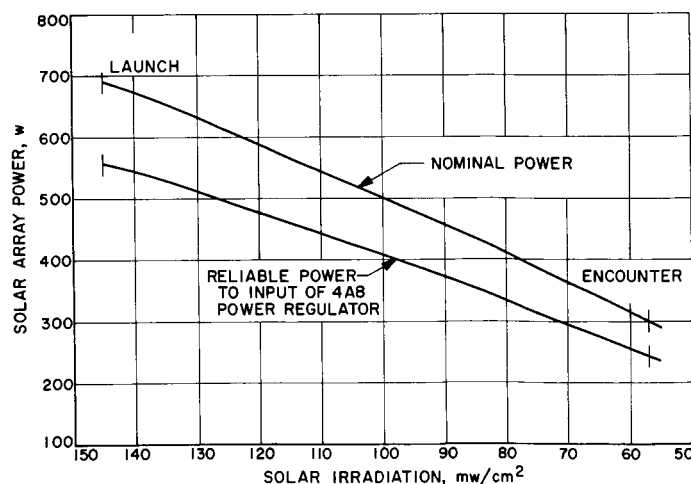

Fig. 10. Solar array power

Fig. 11 shows a functional block diagram of the autopilot subsystem. Three-axis disturbing torques arising from misalignment of the rocket-motor thrust vector act through the spacecraft dynamics to produce rotations about the three spacecraft axes. The gyroscopes sense these rotations and provide the autopilot with voltages
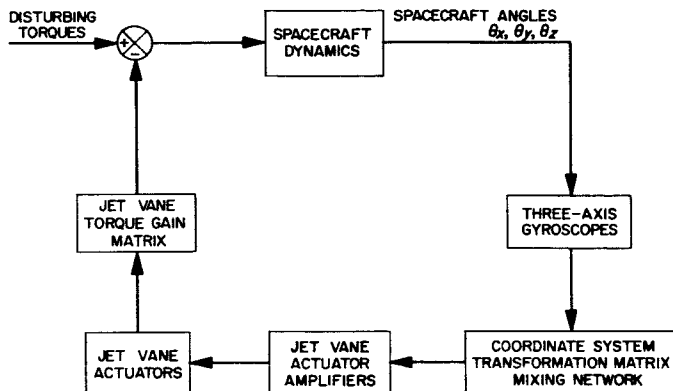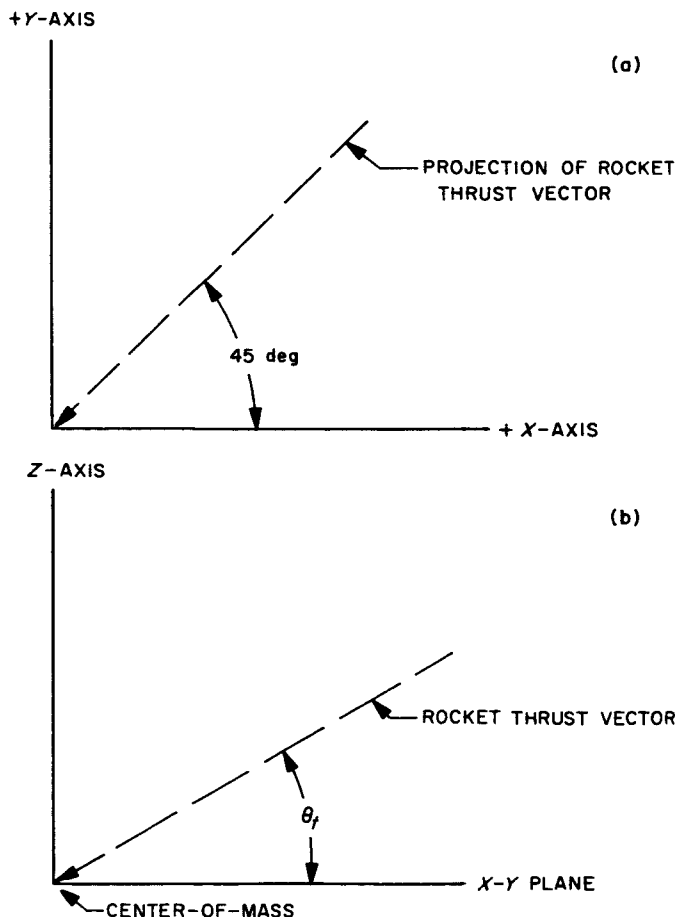

Fig. 11. Autopilot block diagram

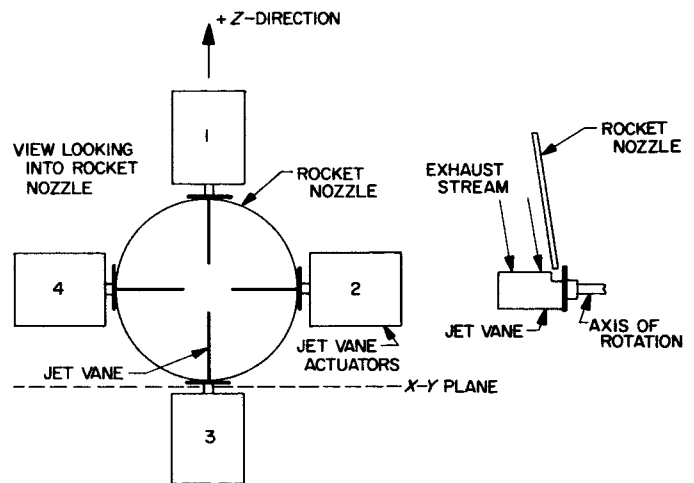**Fig. 12. Rocket thrust vector in spacecraft coordinates**

Fig. 13. Placement of jet vanes on rocket motor

proportional to the spacecraft angular rates and positions. The gyro signals are processed by a mixing network into signals appropriate to a coordinate system natural to the jet vanes, and the jet vane actuator amplifiers use these signals to position the four jet vanes. Forces on the jet vanes are resolved into torques about the spacecraft axes by their geometrical placement.

The rocket motor orientation (Fig. 12) on *Mariner C* has posed some special problems to the autopilot. Fig. 12(a) shows the rocket-motor thrust vector as projected in the spacecraft X-Y plane. Fig. 12(b) shows the thrust vector tilted out of the X-Y plane by a small angle. The motor is tilted in order to point the thrust vector as close as possible to the spacecraft center-of-mass. Fig. 13 shows the arrangement of the four jet vanes, which are mounted in a plane perpendicular to the rocket thrust and located at the exit of the rocket nozzle.

D. Three-Axis Spacecraft Simulator

Spacecraft attitude-control subsystems can be ideally tested only during actual space flight. Environmental parameters that are characteristic of deep space, namely, zero gravitational forces, zero aerodynamic friction, and ultimate vacuum, cannot be duplicated in the laboratory. However, a three-axis air-bearing supported table (Fig. 14) is extremely useful in evaluating the dynamics of attitude-control subsystems.
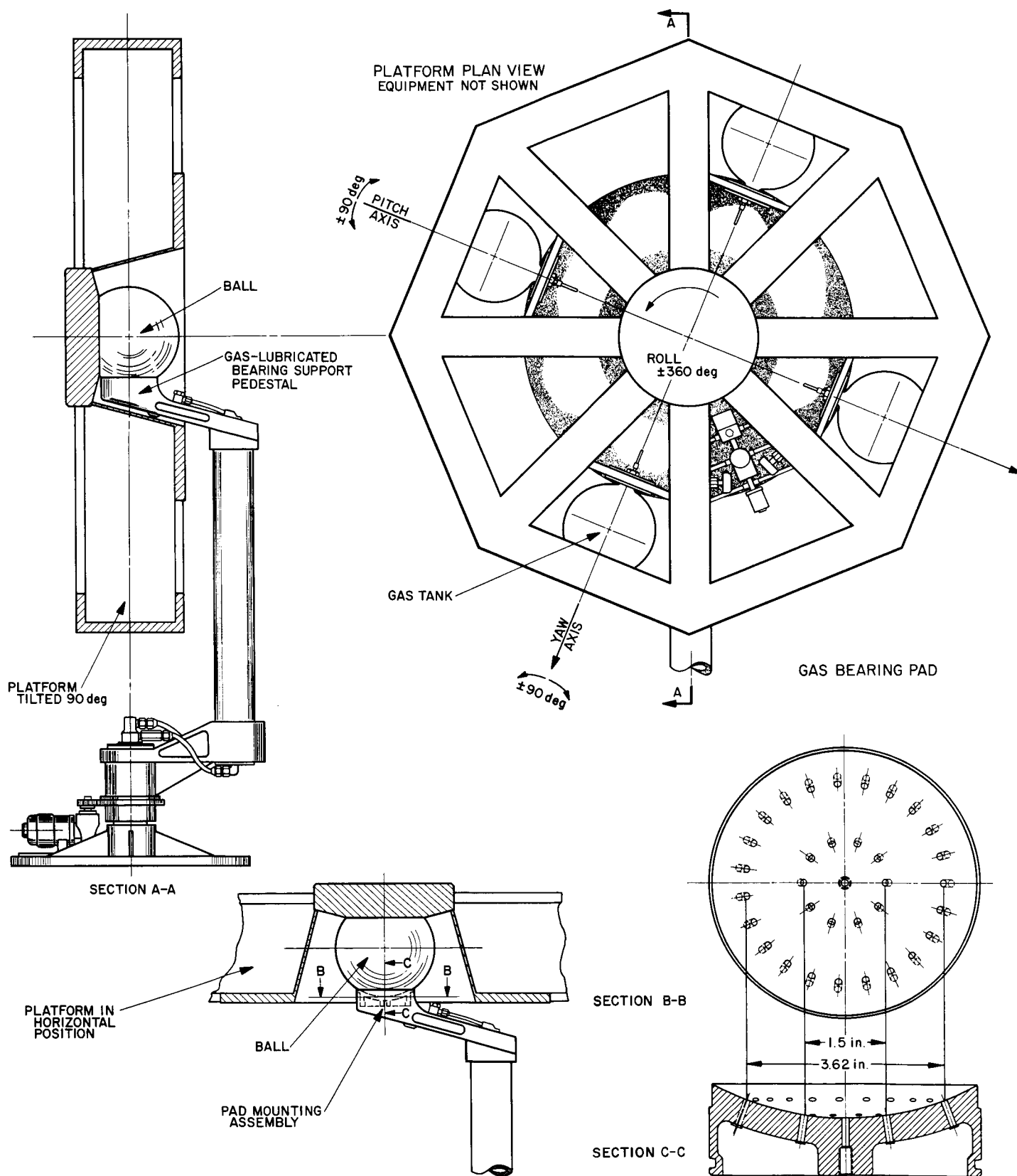
PLATFORM PLAN VIEW
EQUIPMENT NOT SHOWN

±90 deg

PITCH
AXIS

BALL

GAS-LUBRICATED
BEARING SUPPORT
PEDESTAL

ROLL
±360 deg

PLATFORM
TILTED 90 deg

GAS TANK

YAW
AXIS

±90 deg

GAS BEARING PAD

A

SECTION A-A

PLATFORM IN
HORIZONTAL
POSITION

SECTION B-B

BALL

PAD MOUNTING
ASSEMBLY

B   C   B

C

1.5 in.

3.62 in.

SECTION C-C

Fig. 14. Three-axis spacecraft simulator assembly

The simulator table is octagon-shaped and is constructed of stainless steel to minimize deflection torques of a magnetic nature. The table weighs nearly 1800 lb, has a diameter of 60 in., and is approximately 11 in. thick. The air bearing consists of a 10-in.-D beryllium ball that nests in a 5-in.-D matching pad installed in a rigid support pedestal (Fig. 15). A portion of this ball is removed to provide for mounting the octagonal table. The matching pad has two concentric circles of gas jet orifices. These jets are supplied with air under controlled pressure. A nylon ring supports the ball and table when no air pressure is applied. The pad is so constructed that it rises a short distance, as a piston, whenever air pressure is applied. The table is thus lifted or floated by the air coming through the jet orifices in the pad, forming a gas-lubricated bearing.

A basic attitude-control subsystem, which includes gyros, Sun sensors, Canopus sensor, attitude-control electronics module, nitrogen tanks, regulator, and control gas jets, will be mounted upon the table. An automatic balance servosystem is included in the simulator hardware to attain very close balance in all three axes. This automatic servosystem will utilize the flight gyros as sensors.

An RF command subsystem in conjunction with an RF telemetry link allows the spacecraft simulator to be operated with no hard-line connections. Sealed nickel-cadmium batteries supply the simulator power. The cold-gas subsystem for the simulator consists of two identical storage subsystems, a common pressure regulator, and a low-pressure subsystem terminating in the six attitude-control jets. Two jets are used in each axis to produce pitch, yaw, and roll torques. Each storage subsystem consists of two tanks mounted along either the pitch or yaw axis of the sparecraft. Since the two storage subsystems are
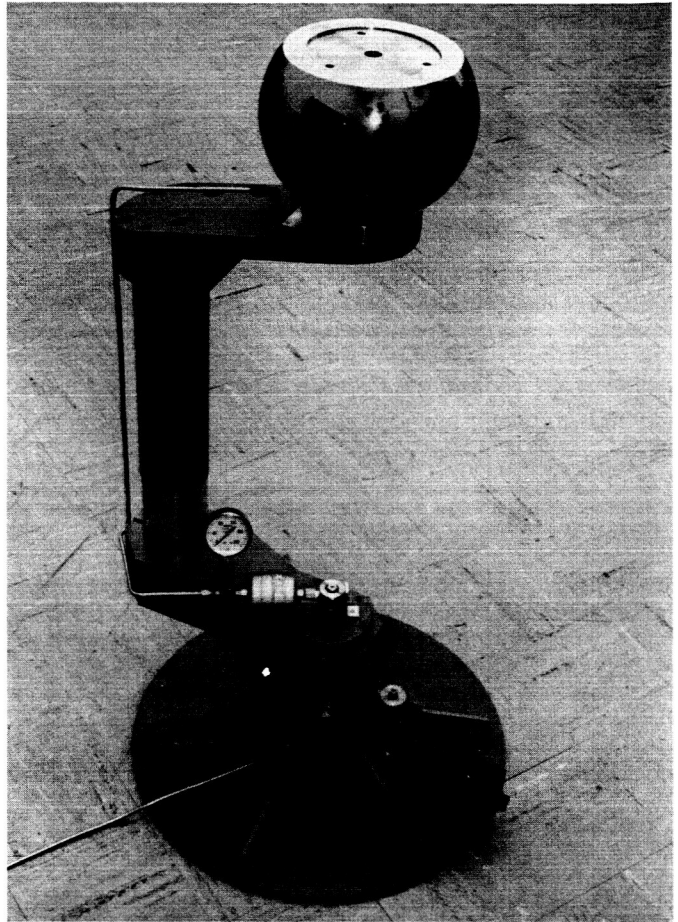

Fig. 15. Air bearing and support pedestal

isolated by valves, it is possible to balance the table for any distortion of the tanks due to pressurization by shifting individual tanks. These tanks are 8.5-in.-ID spheres that were designed for 16,000-psi burst pressure, 6000-psi proof pressure, and 4000-psi working pressure.

THE DEEP SPACE NETWORK

IV. Introduction

The Deep Space Network (DSN) is a precision communication system which is designed to communicate with, and permit control of, spacecraft designed for deep space exploration. The DSN consists of the Deep Space Instrumentation Facility (DSIF), the Space Flight Operations Facility (SFOF), and the DSN Ground Communication System (GCS).

The DSIF utilizes large antennas, low-noise phase-lock receiving systems, and high-power transmitters located at stations positioned approximately 120 deg around the Earth to track, command, and receive data from deep space probes. The overseas stations are generally operated by personnel provided by cooperating agencies in the respective countries while stations within the United States are operated by United States personnel. The names, locations and identification numbers of these DSIF stations are:

Identification No.	Name	Location
11	Goldstone, Pioneer	Goldstone, California
12	Goldstone, Echo	Goldstone, California
13	Goldstone, Venus (R&D station)	Goldstone, California
14	Goldstone, Mars (under construction)	Goldstone, California
41	Woomera	Island Lagoon, Australia
42	Canberra (under construction)	Canberra, Australia
51	Johannesburg	Johannesburg, South Africa
61	Madrid (under construction)	Madrid, Spain
71	Spacecraft monitoring	Cape Kennedy, Florida

The SFOF is located in a three-story building at the Jet Propulsion Laboratory in Pasadena, California, and utilizes operations control consoles, status and operations displays, computers, data processing equipment for analysis of spacecraft performance and space science experiments, and communication facilities to control space flight operations. This control is accomplished by generating trajectories and orbits, and command and control data, from tracking and telemetry data received from the DSIF in near real time. The SFOF also reduces the telemetry, tracking, command, and station performance data recorded by the DSIF into engineering and scientific information for analysis and use by the scientific experimenters and spacecraft engineers.

The DSN Ground Communication System consists of voice, and normal and high data rate teletype circuits provided by the NASA World-Wide Communications Network (NASCOM) between each overseas station and the SFOF, teletype and voice circuits between the SFOF and the Goldstone stations and Cape Kennedy, and a microwave link between the SFOF and Goldstone, provided by the DSN.

The DSN has facilities for simultaneously controlling a newly launched spacecraft and a second one already in flight and, within a few months, will be able to control simultaneously either two newly launched spacecraft

plus two in flight, or the operations of four spacecraft in flight at the same time. The DSIF is equipped with 85-ft antennas having gains of 53 db at 2300 Mc and a system temperature of 55°K, making it possible to receive significant data rates at distances as far as the planet Mars when the spacecraft utilizes directional antennas. To improve the data rate and distance capability of the DSIF, a 210-ft antenna is under construction at the Goldstone Mars Station, and two additional antennas of this size are scheduled for installation at overseas stations. The SFOF has two 7094, two 7040, two 1401, and one SC 4020 computers; four disc files; various input/output units; printers, plotters, and computer interrogation consoles; and teletype, telephone, interphone, public address, and closed circuit television communications systems.

It is the policy of the DSN to continuously conduct research and development of new components and systems and to engineer them into the DSN to maintain a state-of-the-art capability.

The DSN is a NASA Facility, managed by the Jet Propulsion Laboratory through a contract between NASA and the California Institute of Technology. The Office of Tracking and Data Acquisition is the cognizant NASA office.

Sections V and VI that follow are a digest of the information that appears in *SPS 37-27*, Vol. III.

V. The Deep Space Instrumentation Facility

A. Tracking Stations Engineering and Operations

1. Project and System Engineering

a. Ranger *Block III.* During the *Ranger 6* flight, the DSIF stations were directed to record received carrier power level during the period of equal range to the spacecraft. The results of this experiment indicated, after correction and weighting procedures, that in 14 station pair comparisons, the average disagreement in received carrier power measurements was 1.7 db, collective over all the observations. The maximum disagreement was approximately 4 db; most of this discrepancy resulted from a nonstandard RF configuration. The minimum was 0.0 db.

b. Mariner C. A ground transmitter power of 100-kw continuous wave will be required for certain *Mariner C* operations. The complete transmitter program consists of a 100-kw klystron amplifier subassembly, a ground test and checkout facility, and specialized controls for this installation. The finalized amplifier layout in the Cassegrain feed cone is shown in Fig. 1.

The 100-kw Venus site is being prepared for backup support of the *Mariner C* spacecraft. It will be utilized where necessary to interrogate the spacecraft (through the omni-antenna) during the last three months of flight. It will be available on an on-call basis approximately 6 hr after notification. Initial tests of the complete Venus 100-kw site with the *Mariner C* spacecraft are scheduled for February 1965, approximately three months after launch.

c. Suitcase telemetry system. A suitcase telemetry system will be designed to supply telemetry coverage for *Mariner C* spacecraft at downrange locations where no coverage is presently available. The system will be light enough to be carried as luggage by a two-man team. Critical spacecraft events, such as separation, will be monitored. The feasibility and effectiveness of such a station will be determined by attempting to acquire and track the *Mariner C* spacecraft.

For proper coverage, two such stations should be employed, one at Johannesburg and one on Mauritius Island. Each station will consist of an antenna and mount,
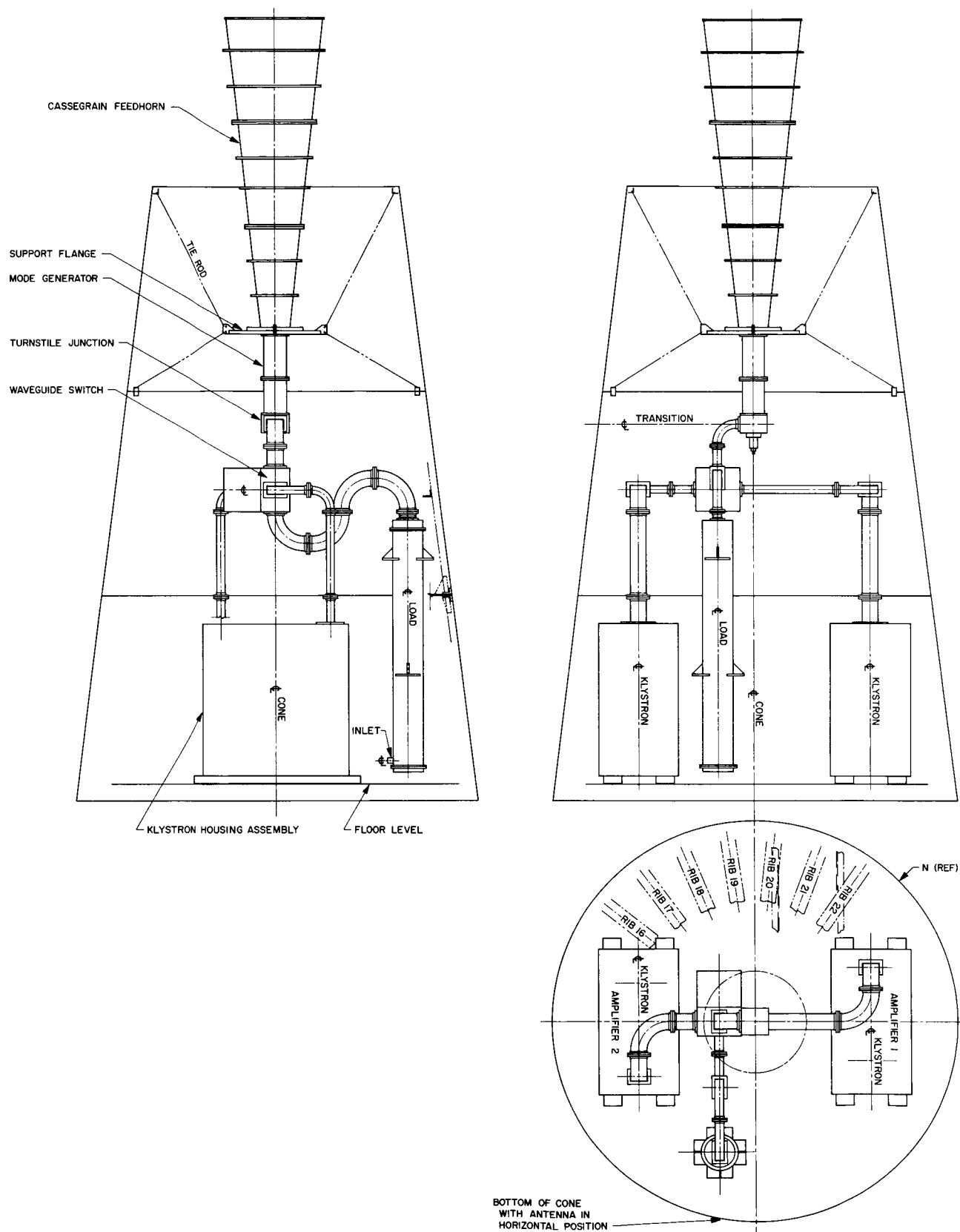
Fig. 1. Final amplifier layout in Cassegrain feed cone

a receiver, a tape recorder, a timing receiver, and associated power supplies.

Initial aircraft tracking tests at Goldstone indicated that a small 2- to 3-ft circular polarized antenna, mounted on a tripod with an azimuth–elevation mount, will probably be satisfactory. A wide beamwidth antenna (15 to 20 deg) is required to facilitate acquisition. The receiver will be a modification of the *Mariner C* spacecraft transponder receiver. The tape recorder employed will record four tracks: two data, one voice, and one time signal.

2. Pioneer Station Operations

With the selection of the Pioneer Station as the installation for the initial operational testing of all DSIF S-band equipment and training of local and overseas personnel, it became necessary to increase the size of facilities there. An interim prefabricated building was erected to house the S-band equipment and to allow equipment testing to proceed on schedule. Two new wings being added to the present control building will permanently house the S-band equipment.

In the standard S-band equipment, the receiver operates at 2295 Mc, with a dual-channel capability of receiv-

ing two spacecraft signals simultaneously. The S-band transmitter (Fig. 2) differs from earlier transmitters in that the exciter has been incorporated with the S-band receiver. This feature provides for grouping of operating controls into a centralized position, allowing closer coordination of transmitter and receiver functions.

The standard S-band system incorporates a traveling wave maser/closed cycle refrigerator. Fig. 3 shows the maser assembly installed in the S-band cone on the Pioneer antenna for testing.

An S-band acquisition aid antenna system mounted on the 85-ft antenna (Fig. 4) provides a broad beam for initial acquisition of the spacecraft. Alignment and testing of the acquisition aid antenna is performed using a folding collimation tower.

Ancillary subsystems, which have been modified for the S-band system, include a data handling subsystem for tracking data handling and angle encoding, and an analog instrumentation subsystem with associated magnetic tape and oscillograph recorders. Mission-dependent (*Mariner C*) ground telemetry equipment is being operationally tested. An Astrodata read, write, and verify ground command subsystem, capable of providing both stored and
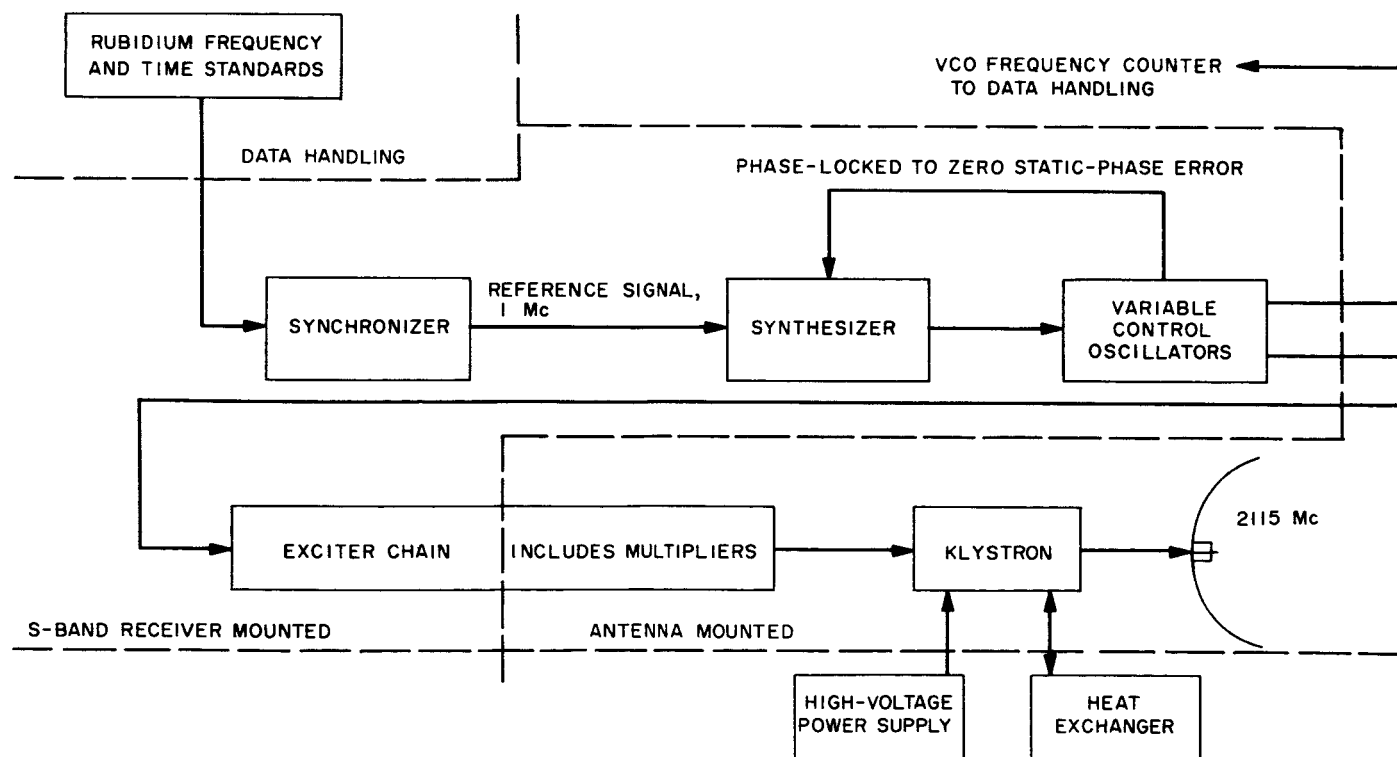

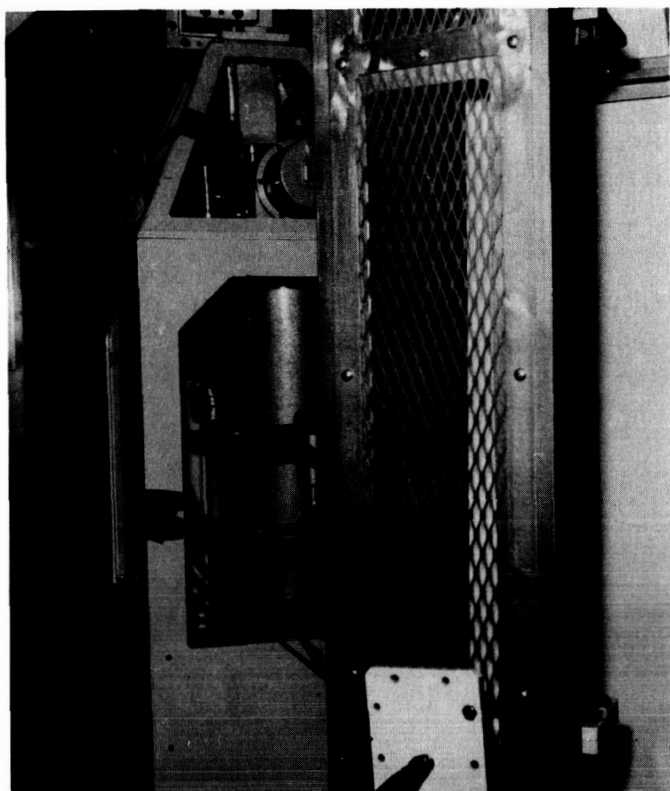Fig. 2. S-band transmitter block diagram

Fig. 3. Traveling wave maser/closed cycle refrigerator in antenna cone

real-time commands to either *Ranger* or *Mariner* spacecraft, is being operationally tested for interface agreement with associated subsystems.

The original L-band receiver has been converted to an L/S-band receiver, operating at either 960 Mc (L-band) or 2295 Mc (S-band). Associated with this receiver is an L/S-band transmitter which provides the required transmission capability. The conversion allows easy changeover to the L-band configuration for use during *Ranger* Block III or similar missions.

3. Antenna Engineering

Modifications and additions to the Pioneer antenna for S-band operation covered: retrofit structural modifications, optical tracking aid system modifications, S-band acquisition aid support hardware installation, 85-ft dish resurfacing, and final alignment.

Retrofit structural modifications included: (1) construction of a two-level weatherproof electronics house in the declination wheel structure, (2) replacement of the
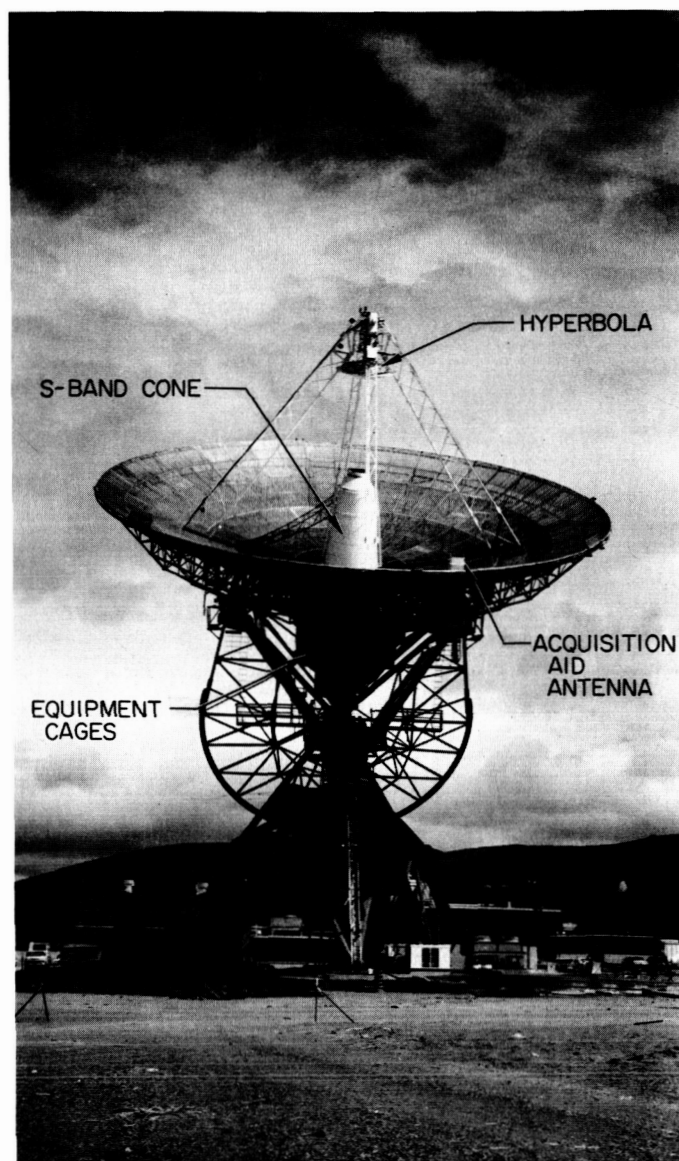

Fig. 4. Pioneer antenna rigged for S-band tracking

old tubular-type quadripod with a truss type of improved strength and stiffness, (3) replacement of the existing L-band Cassegrain cone and hyperbola with an improved S-band Cassegrain cone, and (4) addition of a refrigeration unit (10-ton capacity) and three heat exchanger units in the environmental control system.

Optical tracking aid system modifications (for both the Pioneer and Echo antennas) included: (1) addition of new snap-in mounts for the TV and boresight cameras and lens, (2) addition of event indicators in the boresight camera control unit, (3) replacement of the stepping switch drive in the filter wheel drive mechanism with a dc-motor drive, and (4) separation of the TV controls,

TV filter wheel, and automatic door cover controls into two modular assemblies.

In support of the S-band acquisition aid (SAA) system, the following hardware items were installed:

(1) An optical acquisition aid subsystem, which is a TV camera-lens package (Fig. 5) that enables the servo operator either to boresight the SAA horn on its collimation tower or to track a target such as a helicopter. The system comprises a reference telescope, TV camera and monitor, and a 4-deg field-of-view f2.5 lens.
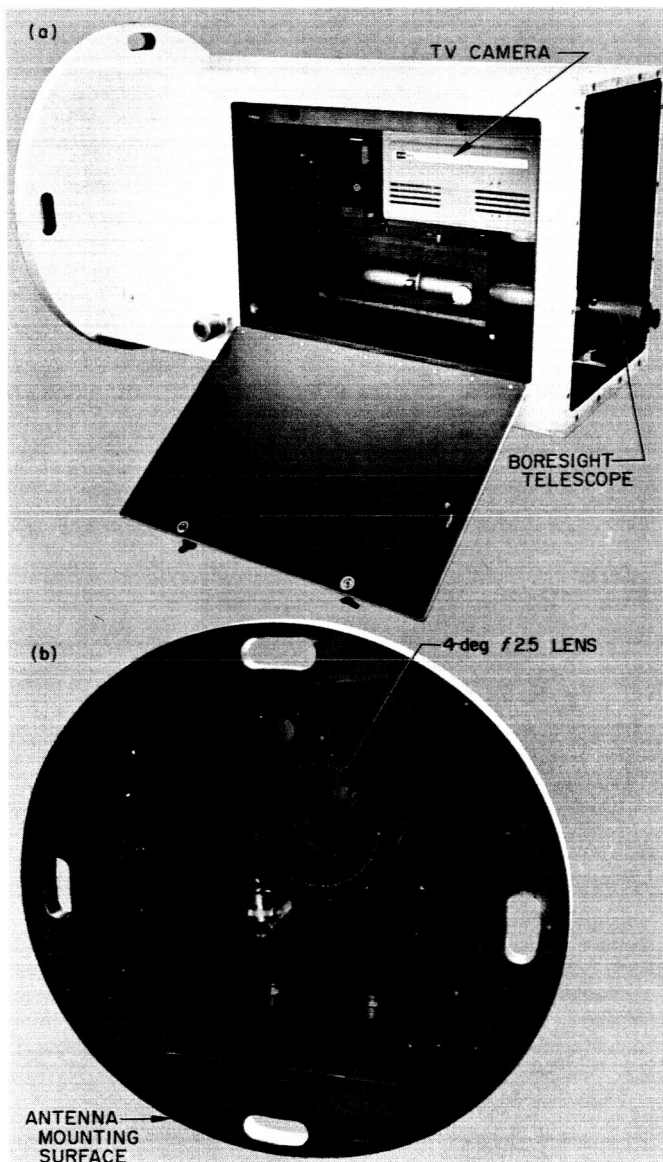
(2) A servo control unit which furnishes the link between the SAA horn end signals and the servo system. The servo system has been supplemented with control and switching circuits for accepting error signals from either the S-band acquisition or tracking receivers. Provision for switching has been made for both the S-band and L/S-band configurations.

(3) A 30-ft-high remote-controlled collimation tower for the SAA system (Fig. 6). The tower normally carries an RF boresight horn in its upper cage. The tower may be raised and lowered automatically or manually.

4. Computer-Controlled Antenna-Positioning System

A computer-controlled antenna-positioning system (Fig. 7) is now being installed at the Goldstone Station Venus site. A small general-purpose computer, with 2000-word memory, paper tape punch, photo reader, and typewriter,

Fig. 5. SAA optical package

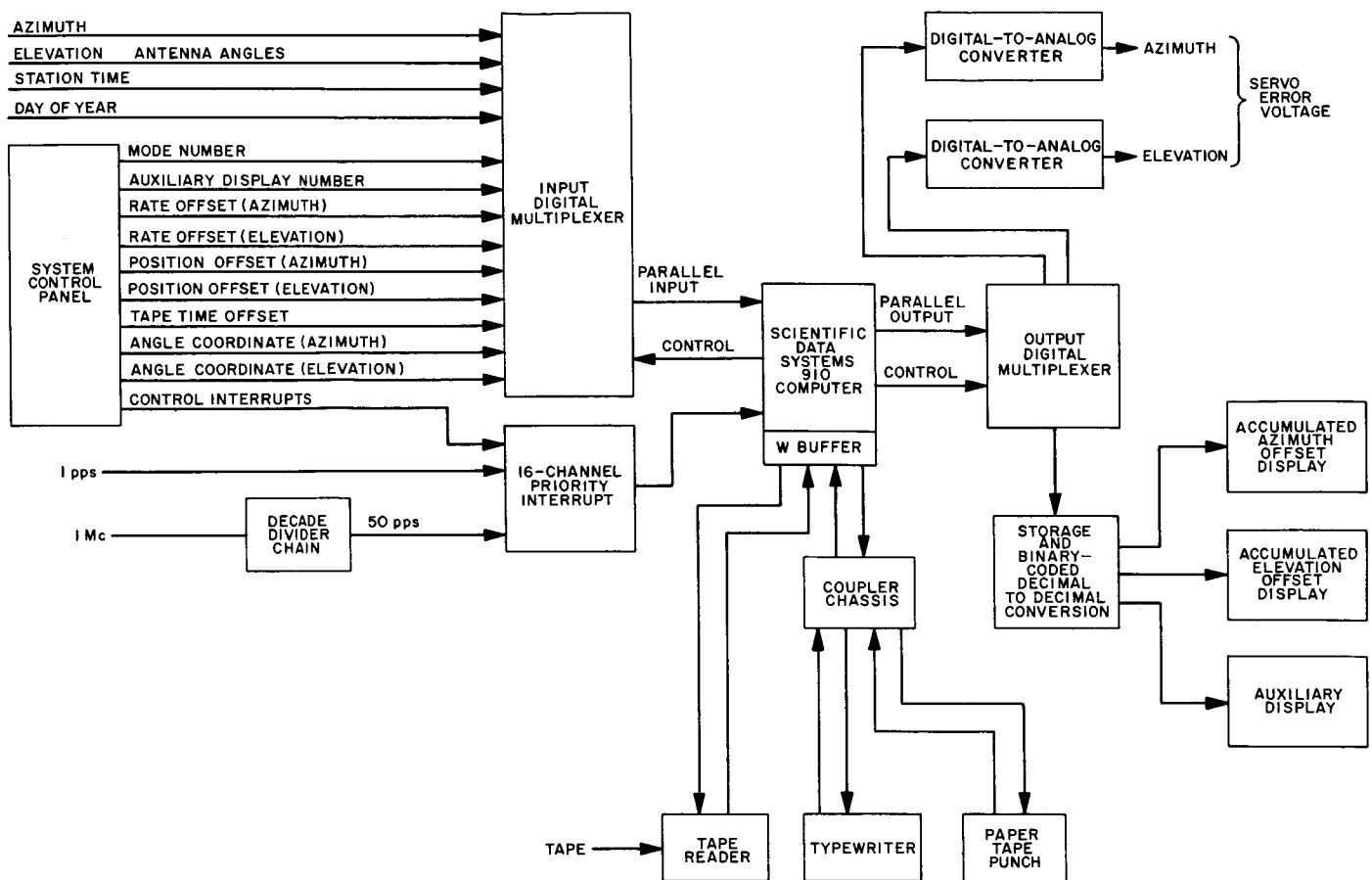Fig. 6. SAA collimation tower in elevated position

Fig. 7. Computer-controlled antenna-positioning system block diagram

will be used in conjunction with special interface equipment to handle as much of the operation as possible, thereby minimizing the amount of peripheral equipment required. This system will be evaluated for eventual use on all stations of the DSIF tracking network.

The system will be enclosed in the servo drive loop on an 85-ft-diameter azimuth–elevation (Az-El) mounted tracking antenna. Inputs of antenna position from the angle encoding system and GMT from the data handling system will be required. In addition, digital inputs from a system control panel will be utilized. Digital-to-analog converters will supply output voltages to the antenna servo system in proportion to the antenna position error. Outputs will be provided for the recording and display of selected functions within the computer. All control of data input–output, comparisons, calculations, error detection, and code conversions will be accomplished by the computer.

Information will be transferred from a system control panel to the computer by actuating push-button inter-

rupts. The interrupts may either command the computer to perform a particular calculation or to read digital information selected on digital switches located on the control panel. Selectable information will include mode number, offsets, and coordinate inputs. Data will be selected in decimal form and converted to a binary format.

5. Mark I Ranging Subsystem

The Mark I ranging subsystem (Fig. 8) is being built to equip the Deep Space Instrumentation Facility with the capability of ranging on spacecraft "turnaround" transponders to distances of 800,000 km.

Design was completed and a prototype was built for laboratory use. This prototype was mated with the S-band test receiver–transmitter at JPL. Helicopter transponder ranging tests were run. These tests confirmed the completeness and accuracy of the design of the ranging subsystem.
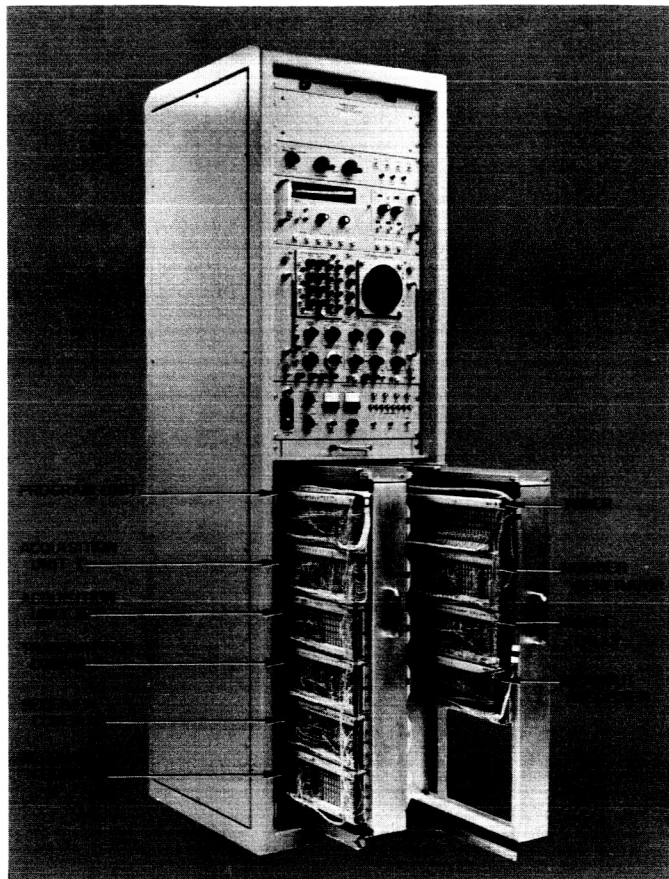
Fig. 8. Mark I ranging subsystem with door removed, showing arrangement of digital assemblies

Construction of the Serial No. 1 (Pioneer) subsystem was completed. This subsystem was installed in the interim S-band control building at Goldstone. It is currently undergoing interface compatibility tests with the S-band radio subsystems and the data handling subsystem.

B. Communications Research and Development

1. Ground Antennas

a. Antenna instrumentation. A transportable instrumentation system is being developed for use in research and development testing of the structural and mechanical properties of large ground antennas. The system will be used initially on the 30- and 85-ft antennas, and later

on the 210-ft-D Advanced Antenna System. The current block diagram of the antenna instrumentation system is shown in Fig. 9. Being designed for use with a specific data system is a general data reduction program which provides low-speed data sampling on punched paper tape records. The program will enable rapid reduction of data from future tests.

b. Radio calibration. Radio astronomy techniques were employed at the Venus site for the calibration of the 85-ft Az-El antenna. The antenna was calibrated for pointing accuracy and effective antenna area by using the signal received by several intense radio sources. In measuring the radiometric quantities, radio-frequency terminations immersed in a cryogenic bath were employed as thermal noise standards.

c. Simultaneous lobing radiometric tracking system. The S-band systems for the DSIF 85-ft and future 210-ft antennas will use simultaneous lobing angle tracking feed systems. A radiometer employed with the tracking feed would be a useful device for angle pointing and gain calibration of the antenna system, using radio star sources. An X-band laboratory demonstration model of a simultaneous lobing radiometer receiver channel was constructed. A noise tube was used to simulate the signal from a radio source. Preliminary experiments were performed to examine the angle detector output versus reference/error channel differential phase shift and error channel noise-to-signal ratio.

2. Lunar/Planetary Radar System

a. Experiments. The Venus site at Goldstone has been used as a field testing laboratory for development of an advanced space communications system and the component technology applicable to the Deep Space Instrumentation Facility (DSIF). Principal activity at the site concerns lunar and planetary radar experiments. The radar experiments involve the same devices as a two-way deep space communications link (excepting an active transponder), e.g., big antennas at high frequency, powerful transmitters, low-noise receivers, and signal processing techniques economical of signal-to-noise ratio. The experiments involve radio propagation over the portion of the solar system of concern to present and near-future space communications, and they involve long and continuous operation of the equipments used. For these reasons, the radar experiments are an effective device for accomplishing some of the advanced technology needed to support the DSIF/JPL space communications work. Also, the

Fig. 9. Antenna instrumentation system block diagram

scientific information obtainable from the radar measurements, e.g., surface characteristics of the Moon and planets and improved determination of their motions and locations, is of use to communications and tracking work.

The experiments performed at the Venus site include: amplitude-modulation signal spectrum and power, continuous-wave signal spectrum, range-gated signal spectrum (mapping), phase-lock receiver doppler velocity on the planet Venus, and lunar ranging. All are active radar experiments. The system is also used in a passive mode as a radiometer to make black-body temperature measurements of Venus, and radio star tracks to establish antenna gain, system temperatures, antenna boresight, and servo pointing accuracies.

b. System description. A functional block diagram of the lunar/planetary radar system is shown in Fig. 10. It is a monostatic time-shared continuous wave (CW) system using an 85-ft antenna for transmitting and receiving on planetary targets. For lunar measurements a separate 6-ft-diameter antenna mounted on the 85-ft antenna quadripod apex is used for receiving. The operating frequency is 2388 Mc.

A 100-kw output CW transmitter is used in three modes of operation: low rate on–off keying, phase modulation, or continuous wave operation. A 1.2-Mw capability 400-cps motor generator provides primary power for the transmitter beam voltage. High-voltage vacuum rectifiers are used to supply the high-voltage dc for the klystron (approximately 32 kv at 8.5 amp). The Cassegrain feed can provide right- or left-hand circular or rotatable linear polarization. The gain of the 85-ft antenna is 54.4 db with a 0.2-db loss in the transmitter waveguide, yielding a net antenna gain of 54.2 db.
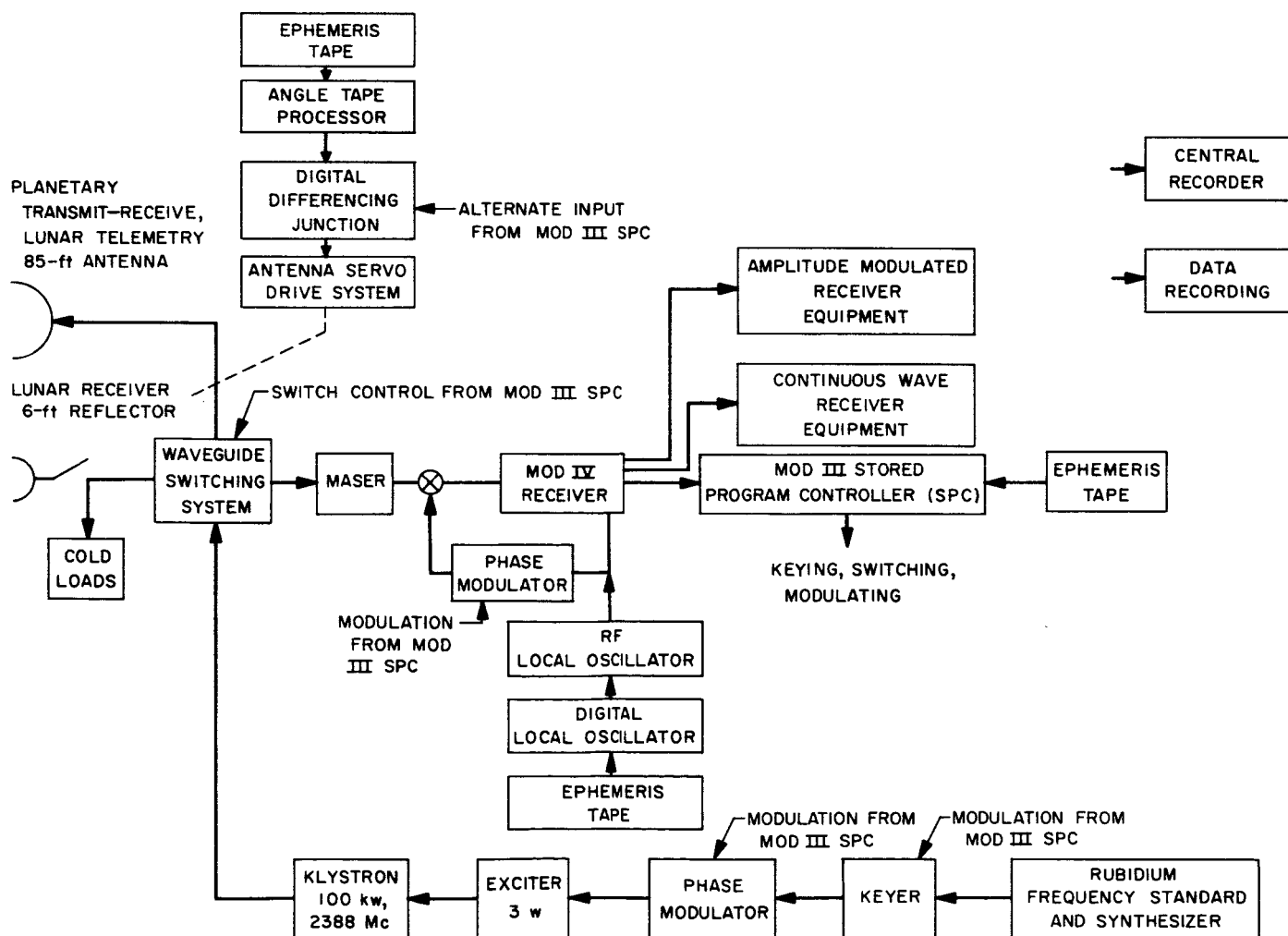

Fig. 10. Lunar/planetary radar system

In the receiving connection, the waveguide losses are 0.1 db; thus, the 85-ft antenna has a net gain of 54.3 db. First amplification of the signal is in a traveling wave maser using a closed-cycle helium refrigerator system operating at approximately 4.4°K. The gain of the maser is approximately 40 db; the total system noise temperature with the antenna at zenith is approximately 29°K. After amplification in the maser, the signals are fed to the Mod IV receiver, a multichannel phase-lock loop receiver used to condition the signal for processing and analysis in the amplitude-modulated, CW, and ranging terminal equipments. The receiver threshold for synchronous operation in a 10-cps noise bandwidth loop is approximately −176 dbm. When the transmitter is on, the receiver is switched into a nitrogen or a helium cold load. When the receiver is on, the transmitter is switched into an RF water load and the RF drive to the klystron is turned off. All of this RF switching is done by large low-loss waveguide switches which can be manually switched by an operator in the control building or automatically switched by command from the ephemeris-controlled Mod III stored program controller (SPC) equipment. The antenna can be steered by manual control with the aid of a closed-circuit television system with an antenna-mounted boresight telescope, or it can be driven in an automatic slave mode from ephemeris data fed into the digital control system.

The Mod III stored program controller is used to control the operation of the radar system in both the lunar and planetary modes. The SPC is supplied with range ephemeris information on punched paper tape for the planetary mode, and with both range and angle ephemeris information for the lunar mode. The time between samples on the planetary range tape has recently been increased from 8 to 60 sec; a linear interpolation is made between sample points. This reduction of sample points has resulted in a considerable saving of time and expense in tape preparation and editing without compromising the accuracy of the range ephemeris.

In lunar and planetary ranging experiments, the SPC is used to control coders which phase-modulate the transmitter and receiver local oscillator. The coder for the lunar mode is a pseudonoise (PN) code generator of length 16,383 with a fixed digit period of 1 μsec. The coder for the planetary mode is a PN code generator of length 511 with a digit period of 125N, where N may range from 1 to 2^{22} μsec. The planetary mapping experi-
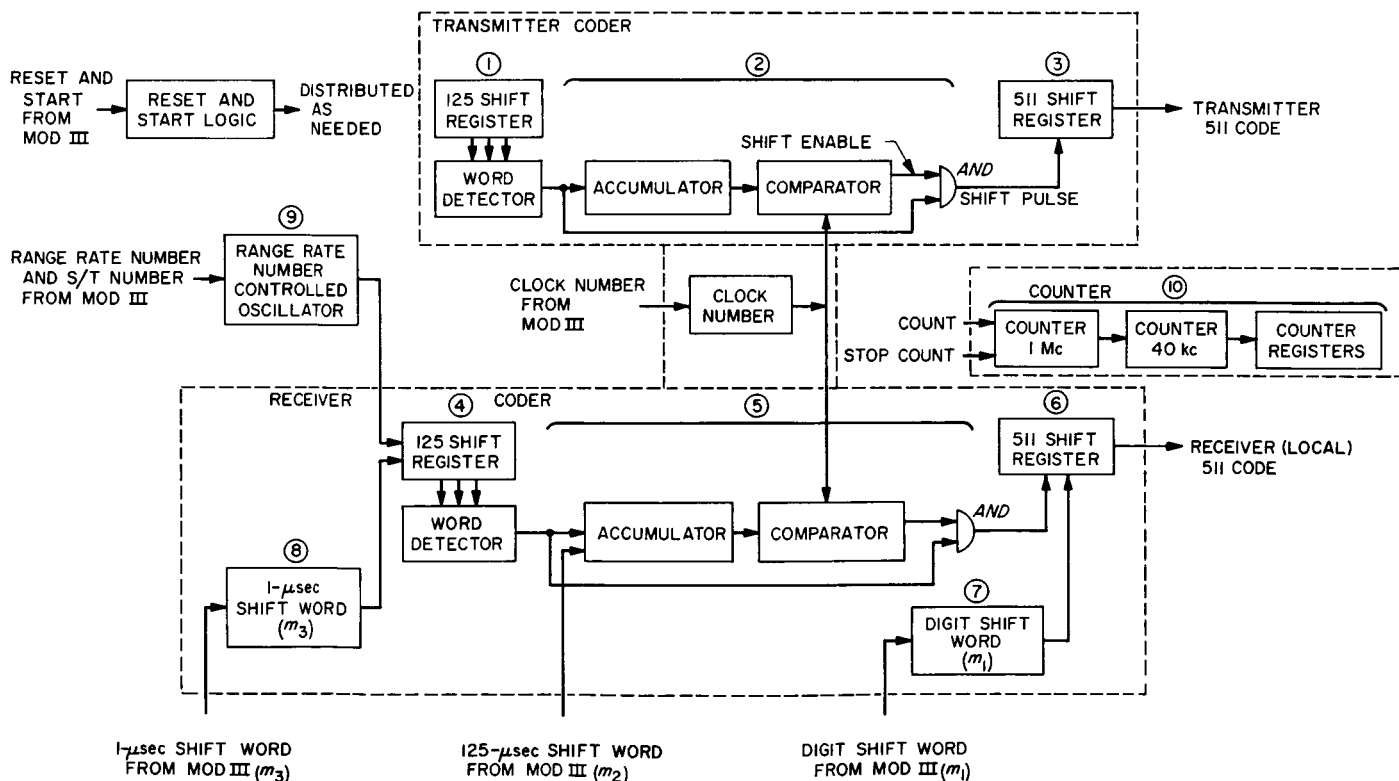

Fig. 11. Planetary ranging coder subsystem block diagram

ment (a technique for doing spectral analysis of a range-gated signal) uses the 511-length coders to phase-modulate the transmitter and demodulate the received signal. In all these experiments, the receiver coder is displaced from the transmitter coder by the ephemeris range delay.

In all experiments except the lunar radar, an angle ephemeris paper tape with samples every 64 sec is used to supply information to the angle tape processor (ATP). The ATP supplies information to the digital differencing junction (DDJ) in the same format as that used when information is sent over the microwave link from the coordinate converter computer at the Echo Station. The DDJ compares the ephemeris angles with the antenna position angles and provides an appropriate error signal to control the antenna servosystem. In the lunar radar mode, an ephemeris paper tape with samples of range and angles every 64 sec supplies information to the SPC. A buffer has been constructed to allow the SPC to supply the angle information to the DDJ directly in the same format as the ATP and microwave link.

In the planetary amplitude-modulation receiver experiment with the single-channel correlator, the SPC is used to modulate the transmitter with a square wave which turns the transmitter on every even second and off every odd second. This technique of synchronizing the keying rate to real time allows the computer to be restarted in the event of power failure without the loss of an entire transmit–receive cycle. The same square wave used to modulate the transmitter is supplied to the single channel correlator displaced by the ephemeris range delay. The SPC also supplies a transmit–receive signal to the single-channel correlator which automatically stops accumulation at the end of the receive cycle.

In all of the experiments, the SPC is used to automatically switch the system from the transmit to the receive mode by means of relays which are program addressable. The length of the transmit or receive cycle is controlled by the range number on the ephemeris tape. A guard delay of 8 sec is used between transmit and receive to allow for mechanical switching of the waveguide switches.

3. Planetary Ranging Coders

A subsystem of planetary ranging coders has been designed and constructed for installation into the Mod III ranging equipment at Goldstone. A block diagram of the coder subsystem is shown in Fig. 11. The various blocks have been grouped into four major units: transmitter

coder, receiver coder, range rate number controlled oscillator, and counter. Basically, the coder subsystem provides two identical pseudonoise (PN) code signals. One of these is used to modulate a transmitted carrier, and the other is used as a local signal in the receiver for correlation detection of the received signal.

4. X-Band Radar System

A new monostatic CW X-band (8448 Mc) radar system is being designed for the 30-ft Az-El antenna at the Goldstone Venus site (Figs. 12 and 13). The system will be capable of performing precision lunar range-gate radar experiments and providing coarse-tracking of the lunar surface to further reduce uncertainty in present lunar ephemerides. This tracking mode will be accomplished by biphase modulation of the transmitter and receiver local oscillators at low digit rates, the return being correlated against two adjacent code phases. The difference between these two correlations will provide the error-tracking curve.

The 30-ft antenna system will give the Deep Space Network extended capability for research and advanced
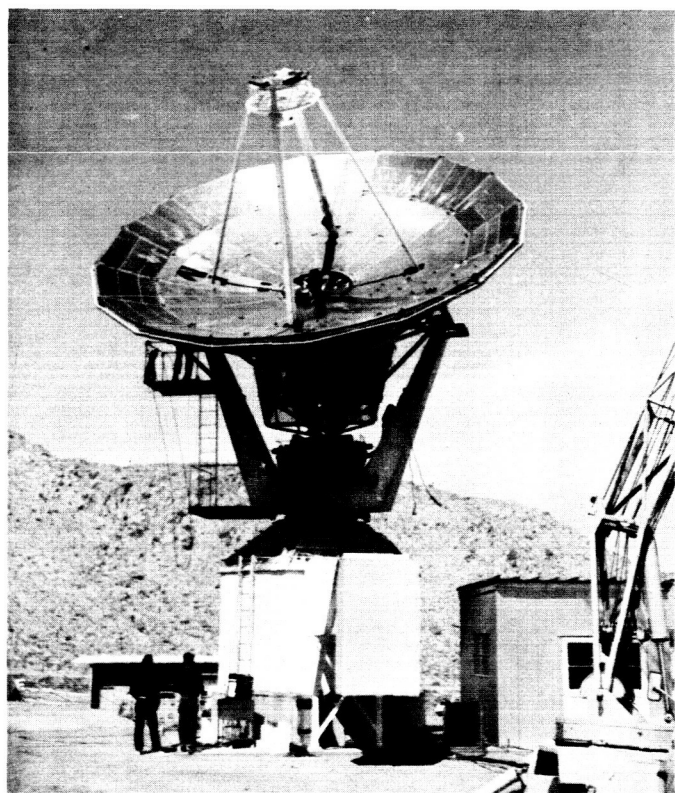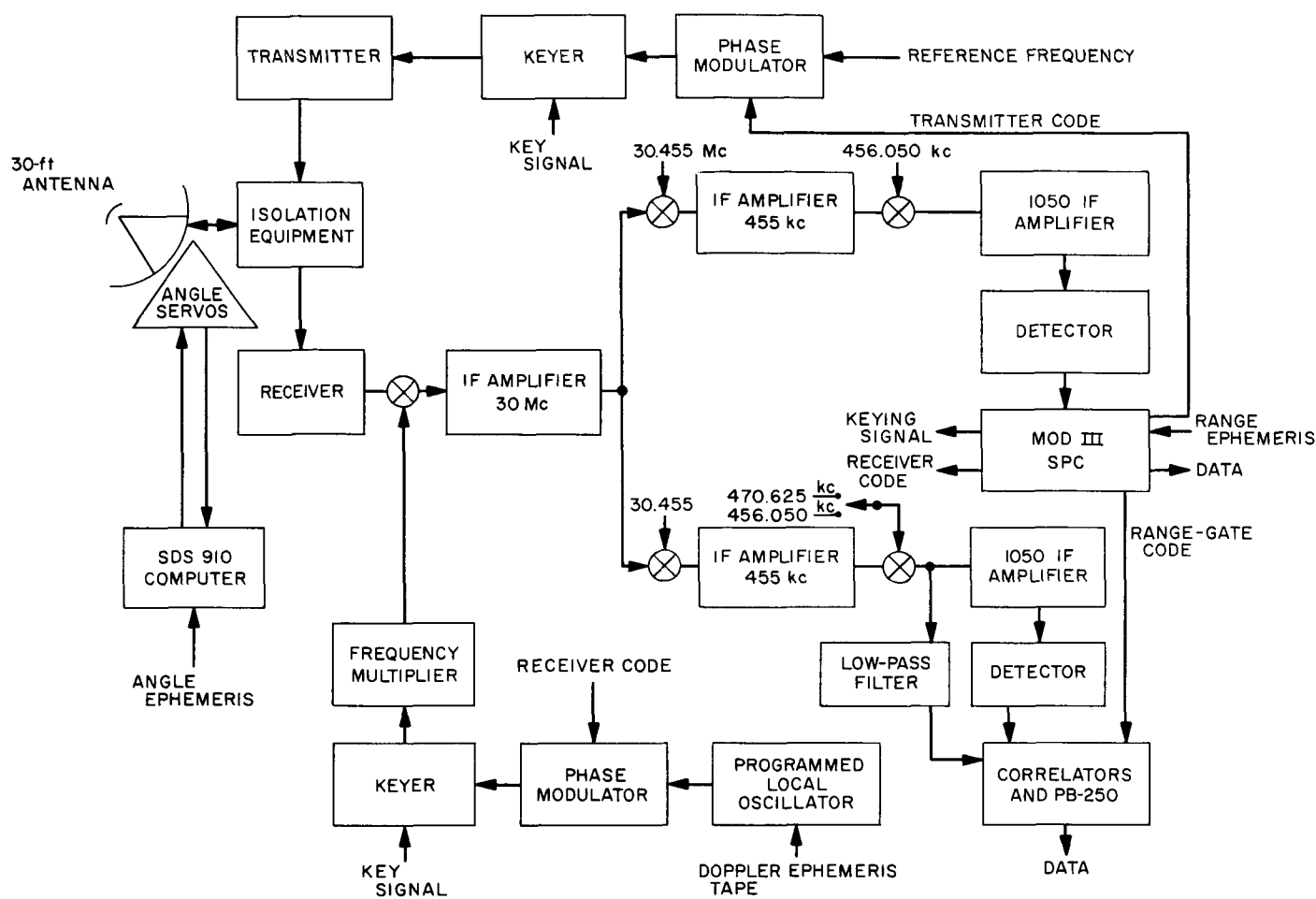

Fig. 12. 30-ft Az-El antenna

Fig. 13. X-Band lunar/planetary radar functional diagram

development. The X-band radar will extend the frequency range of experimental and theoretical space communication studies so that, together with the continuing 2.388-Gc work, the range of radio frequencies of probable future interest in Earth-space-Earth communications will be essentially encompassed.

5. Telemetry System Development

A punctured cyclic coder, a device for encoding and decoding a fixed number k of binary data symbols into any of the nontrivial (n,k) $(n \leq 2^k - 1)$ linear codes which exist for that k, is being built. A study was performed which analyzes such a coder–decoder, for $k = 6$ information bits.

An engineering prototype of a digital machine for computing quantiles on board a spacecraft will be built. The system allows the reconstruction of histograms, previously generated on board a spacecraft, from the values

of only a few sample quantiles, or percentage points, of the histogram. Large data compression ratios, coupled with high statistical efficiencies, have been found.

A random pulse generator will be built for use both as a data source in advanced engineering projects involving compression of data for space telemetry, and as a source of noise for demonstrating coding schemes. As a data source, it will be used to demonstrate the quantile system of data compression. As a noise source, it will be used to generate a burst-error channel for demonstrating the punctured cyclic coding–decoding scheme.

6. Voltage Multiplexer for Stored Program Controller

Many of the tasks to be performed by either the Mod II or III stored program controller (SPC) require the ability to sample an analog voltage, converting the measurement

to a number which the arithmetic unit can process. In transponder ranging operations, the SPC monitors the correlation output of the receiver as the ranging coders are shifted during the acquisition procedure. In RF acquisition experiments, the SPC uses the output of a strong-signal discriminator to guide its operations during the acquisition of the down-link signal, and then applies digital filtering techniques to the ground receiver's static phase error output to assist in recognition of the transponder's acquisition of the up-link signal.

The device used to perform these tasks is an analog-to-digital converter (ADC) which is capable of converting a voltage into a number consisting of ten binary digits and sign, performing the conversion in approximately 50 μsec. The SPC makes use of the ADC by triggering it once for each order the machine performs, doing this at such a time that if the next order asks for a number from the ADC, the number is immediately available. The ADC includes a sample-and-hold input amplifier so that each conversion is performed on a precisely-timed sample of the input signal.

In lunar radar experiments the SPC will have to read several instruments (three or more) in rapid succession, determine which readings are within the scale limits for the instruments, and feed the proper values into the control and data processing programs. To accomplish these operations, the single analog input of the ADC is switched electronically from one channel to another, i.e., selected voltages are multiplexed into the ADC input. A 10-channel multiplexer was installed in the Mod II stored program controller ADC. This unit has been tested and will be installed in Mod III.

C. Advanced Antenna System

A 210-ft-diameter Advanced Antenna System (AAS) is being designed and constructed for the Mars Station at Goldstone. This AAS is designed specifically for deep space communications and will be integrated with related systems and equipment at the Goldstone Station of the Deep Space Instrumentation Facility (DSIF). The antenna will operate initially at the S-band frequencies of 2.1 to 2.3 Gc. The erection of the pedestal and the final design of the basic antenna have been nearly completed. Work has begun on the integrated power system for the AAS. Preliminary design and specification work has been done on the precision data system, including the master equatorial instrument.

The precision angle data system (Fig. 14) will be used to determine the angular position of the antenna beam. To overcome the structural deflection and alignment problems associated with on-axis encoders, optical links are used to measure the angular orientation of the center core of the reflector structure with respect to a ground referenced instrument, the master equatorial (ME). The angular orientation of the reflector structure is represented by the intermediate reference structure (IRS).

There will be two basic modes of precision operation for the AAS, RF auto track and pointing. In the RF auto track mode, the antenna is servoed to follow the RF signal from the spacecraft. To provide precision readout of the beam position in the RF auto track mode, the ME is slaved by means of the optical link and the IRS to the reflector orientation. In pointing modes, the process is reversed; the ME is commanded in hour angle–declination coordinates and the antenna is slaved to it.
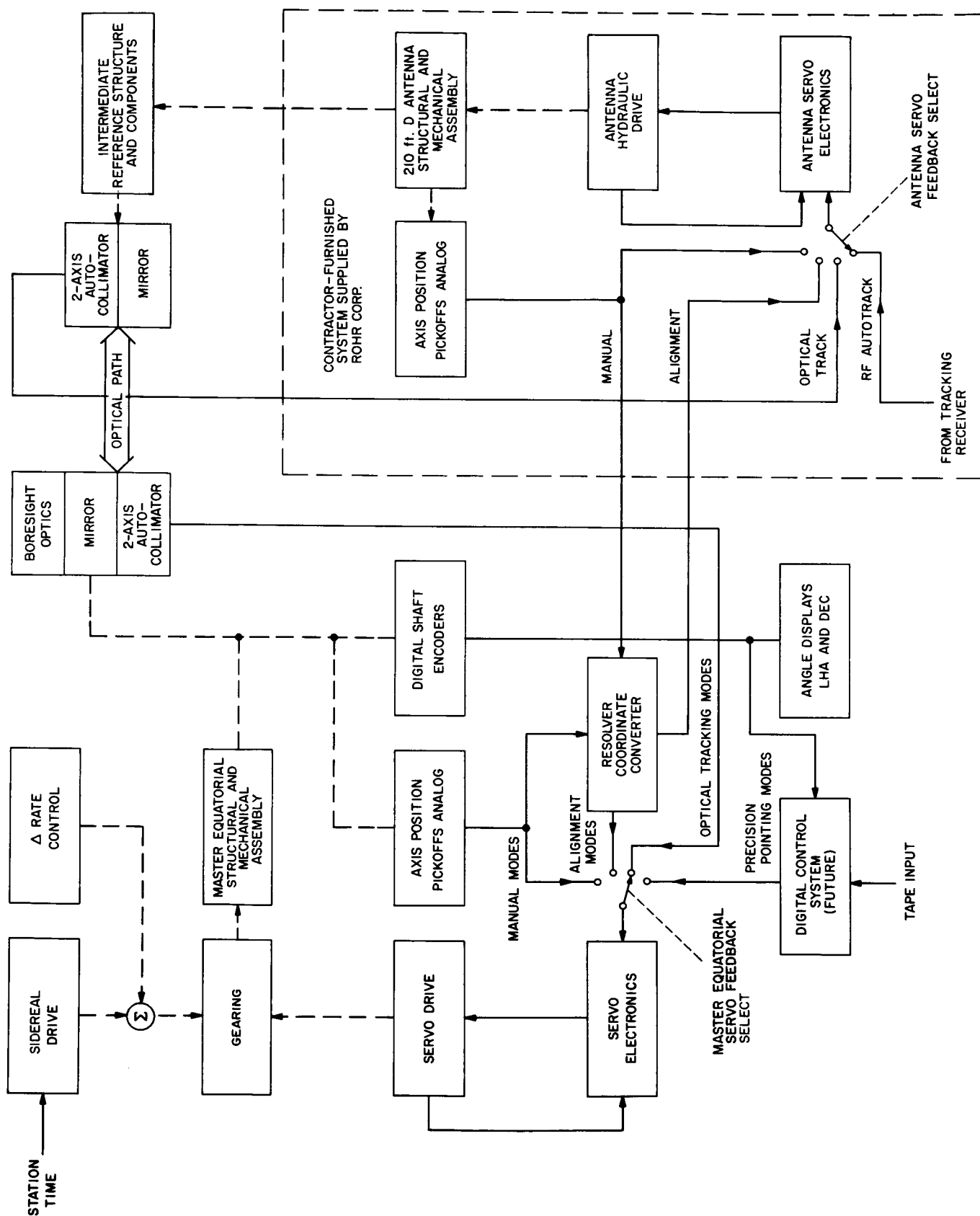
Fig. 14. AAS precision angle data system simplified block diagram

VI. Space Flight Operations Facility

A. Mission Status Board

The mission status board, located in the operations area of the Space Flight Operations Facility, is capable of displaying summary information for two simultaneous missions. Contained in the mission status board are three unique display devices: the Eidophor television projector, the mission events display projector, and various relatively simple semiautomatic displays.

The Eidophor television projector is shown in Fig. 1. The bright picture projected by the Eidophor derives the light not from the conventional projection cathode ray tube, but from a powerful Xenon arc lamp (1.6 kw). The projected picture is of such size and brightness that it is comparable to those produced on a cinema screen. Light from the arc lamp is thrown via mirrors into the Eidophor onto a thin film of oil on which is impressed an electrostatic image of the picture to be projected. This electrostatic image causes local deformations on the oil film which, being strongly illuminated, is capable of being projected by an optical system onto a rear projection screen.

The display projector will show a continuous real-time relationship between event information and current time in each of the selectable time scales. The display employs dual independent projectors. The top projector, called the static unit, has a 7.6- × 10-in. field producing a bright
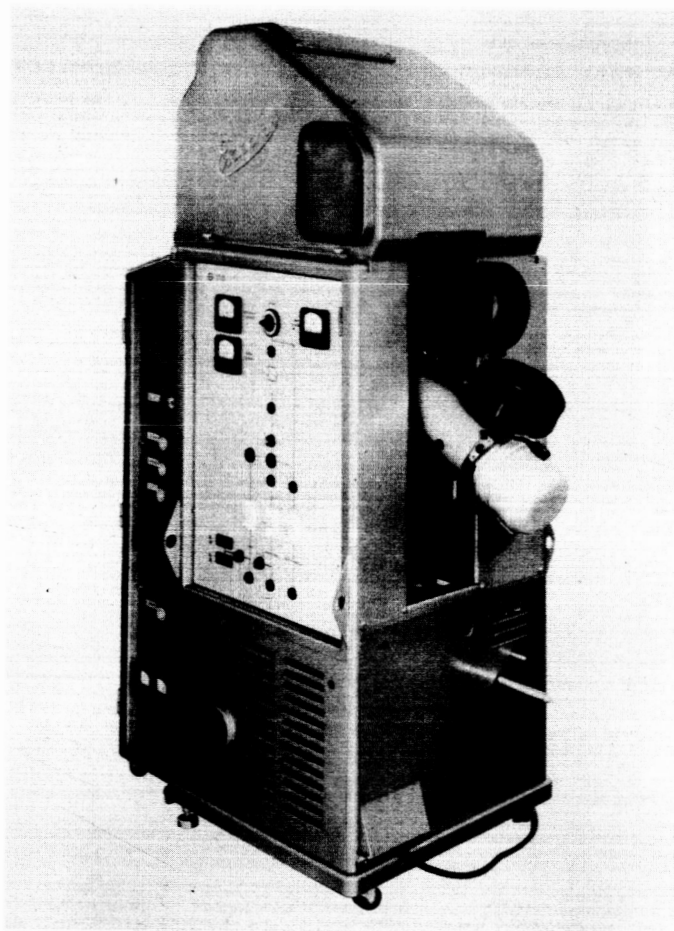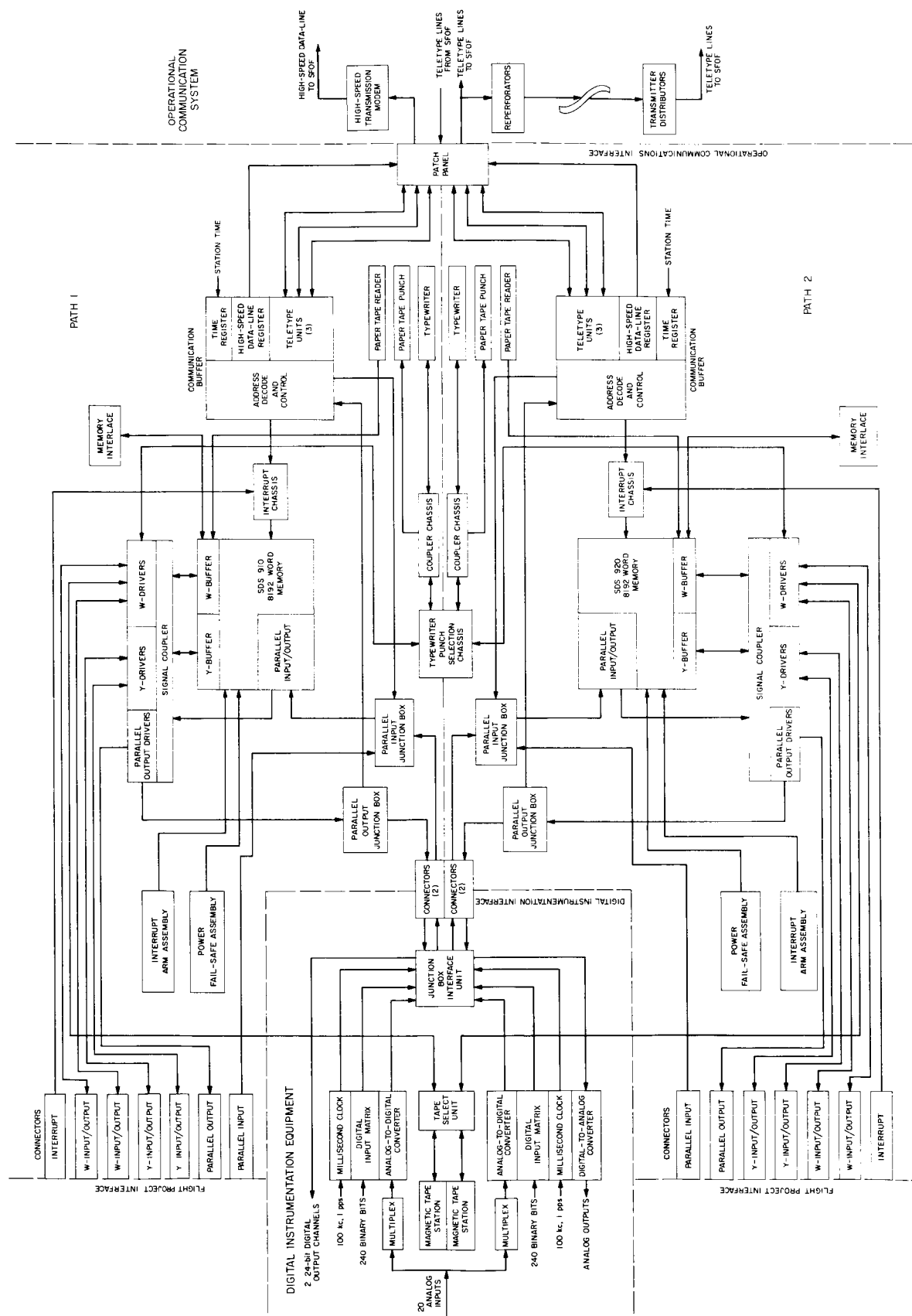

Fig. 1. Eidophor television projector

Fig. 2. Deep Space Network data processing system

66.5- × 88-in. image of the mission event data and symbology. The lower projector, referred to as the cursor unit, is also based upon the same aperture, and generates selectable time cursor sweeps at rates of 1 in./min, 1 in./hr, and 1 in./day.

The image/object geometries are similar to those of conventional high-quality opaque and transparency projectors. The composite image is synthesized or optically mixed by back illumination of a high efficiency, diffused, rear projection transmissive screen. Symbology and alphanumeric characters are projected as high brilliance images on a black background; the cursor image appears as a bright vertical line. The cursor projector slews the cursor image at a uniform timing rate, corresponding to the selected mission event period. A remote control box controls rate selection, cursor positioning rapid slew, cursor intensity, and on-off switches. A flexible display platen permits the rapid updating of the specific data to reflect changes in mission content and/or sequences.

The semiautomatic display modules, approximately 7 ft high, 3 ft wide, and 1 ft deep, are made of light aluminum angle-framing and hard-faced masonite. The names of parameters, items, sensors, and their units or dimensions are prepared on nameplates prior to or during a mission by using pressure-sensitive letters or symbols. The minimum letter size is 1¼ in., which can be viewed at maximum distance of 40 ft. A display control assembly controls the numeral and symbol indicators (digital data indicators) and the condition lights on the module. The control assembly is capable of entering the variable information in any row, one row at a time.

B. On-Site Data Processing System

Preliminary design of the Deep Space Network (DSN) on-site data processing system was completed. The purpose of the system is to provide standardized general purpose digital computing facilities at the deep space stations in order to process spacecraft telemetry data, spacecraft command data, and station instrumentation data.

A block diagram of the on-site data processing system is shown in Fig. 2. The system contains two virtually independent sets of equipment. Each includes a general purpose digital computer, a communications buffer, and input-output peripheral equipment. The duplicate sets of equipment are arranged to provide two on-line data processing paths.

VII. DSN Ground Communication System

A. High-Speed Data Communications System

The need to transmit telemetry data which has been received at Deep Space Instrumentation Facility (DSIF) stations from advanced spacecraft at relatively high bit rates to the Space Flight Operations Facility (SFOF) for real-time analysis has generated a requirement for the development of a Deep Space Network (DSN) high-speed data communications system.

Voice-grade communications circuits with nominal 3-kc bandwidths were selected for the DSN system because these circuits generally are available nationally and can normally be provided internationally. Some form of modulation is necessary to place the information to be transmitted within the useful spectrum of available transmission facilities. A differentially coherent phase-shift keying system was selected to provide the modulation required.

Two types of high-speed data transmission keyers and receivers will be installed in the system. Type I equipment is capable of operation at any of the following switch-selectable data transmission rates: 137.5, 550, 600, 1100, 1200, or 2400 bits/sec. Type II equipment is functionally similar but capable of operation at 2200 or 4400 bits/sec over appropriate transmission facilities.

The transmission keyer (transmitter) units (Fig. 1) utilize 180-deg phase-reversal modulation of a carrier signal and a special data coding translation technique. The coding translation technique permits the transmission of purely random input data as particularly chosen, restricted combinations of logic *ones* and *zeros*. The transmission receivers (Fig. 2) employ synchronous detection and differentially coherent phase comparison techniques.

The basic timing control for the transmission keyers is provided by a stable 76.8-kc crystal oscillator. The output of the crystal oscillator is divided to the required frequencies for the carrier signal, 9-bit timing, and bit-rate timing. Actual data timing either can be accepted from an external timing source or be provided by the keyer to the external equipment.

The transmission keyers and receivers are equipped with integral test facilities (ITF). During periods when the equipment is not transmitting operational data, the units can be placed in the test mode by manually actuating a front panel *operate/test* switch. The ITF capability will be most useful for aligning and evaluating system operation.
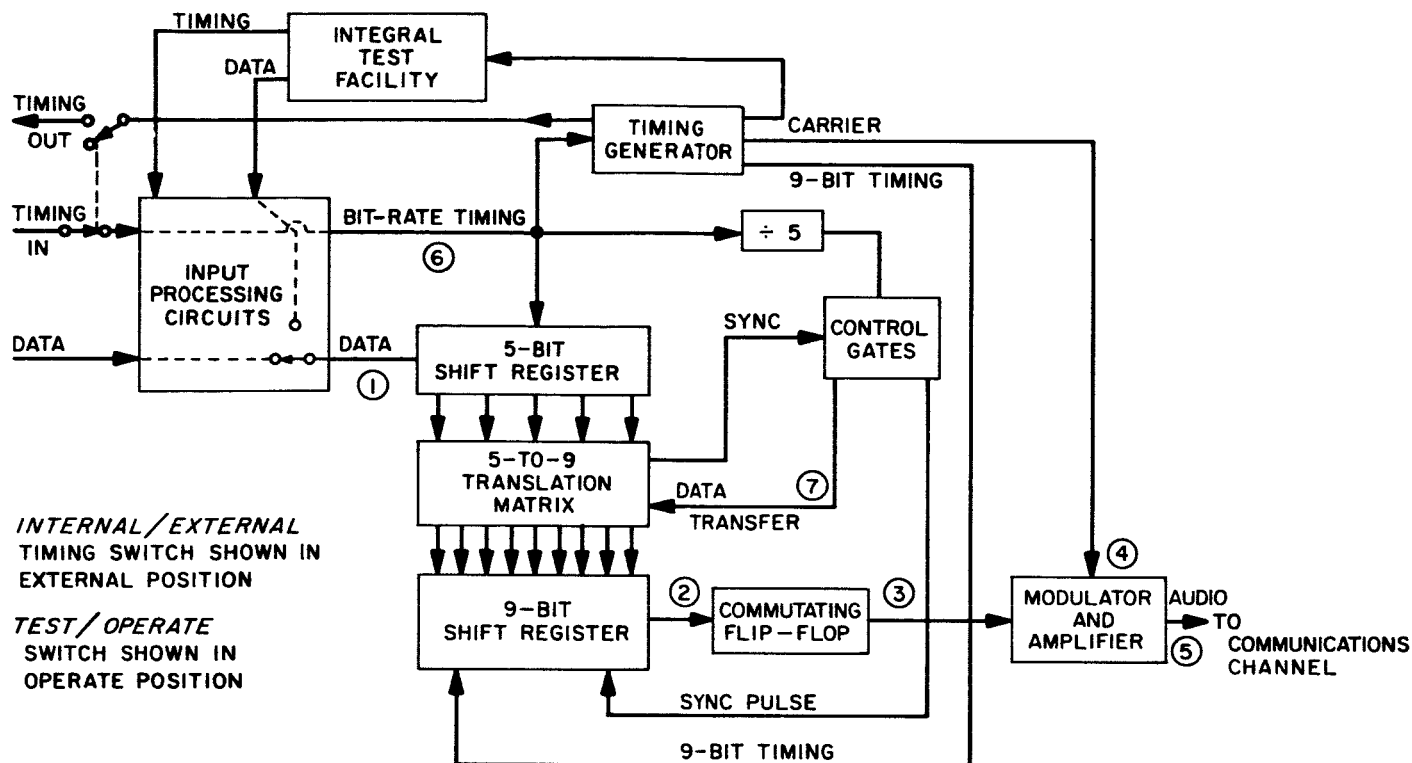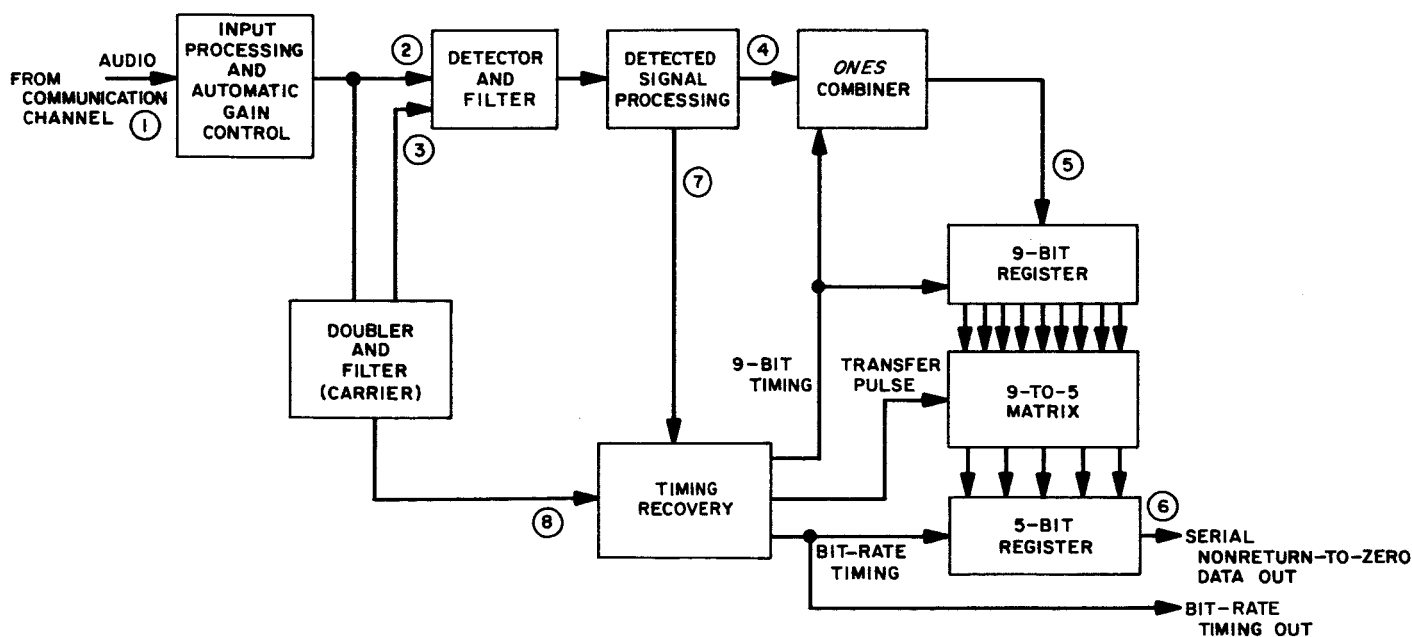
Fig. 1. Transmitter unit

INTERNAL/EXTERNAL
TIMING SWITCH SHOWN IN
EXTERNAL POSITION

TEST/OPERATE
SWITCH SHOWN IN
OPERATE POSITION

Fig. 2. Receiver unit

In the initial configuration of the DSN high-speed data communication system, at least one transmission keyer will be installed at each DSIF station, in JPL facilities at the Atlantic Missile Range (AMR), in the Spacecraft Assembly Facility (SAF), in the SFOF, and one unit will be available for installation at major spacecraft contractor facilities. A special system configuration will be utilized for communication from the DSIF station at Johannesburg, South Africa, because high-frequency radio is required as the transmission medium for a major portion of that circuit. In those cases where a second unit is installed at a DSIF station, the second unit will be an operational spare.

Three Type I receivers will be installed at the SFOF and one at Goldstone DSIF. One Type II transmission keyer will be installed at the Goldstone Pioneer DSIF station and a corresponding Type II receiver will be installed at the SFOF. The latter units will utilize a 6-kc program channel of the Pasadena-Goldstone microwave system at the transmission facility. Five line equalizer units will also be installed at the SFOF to provide a means of improving the data signal conditioning of circuits derived from facilities other than the microwave system. A block diagram of the internal SFOF high-speed data communications subsystem is shown in Fig. 3.
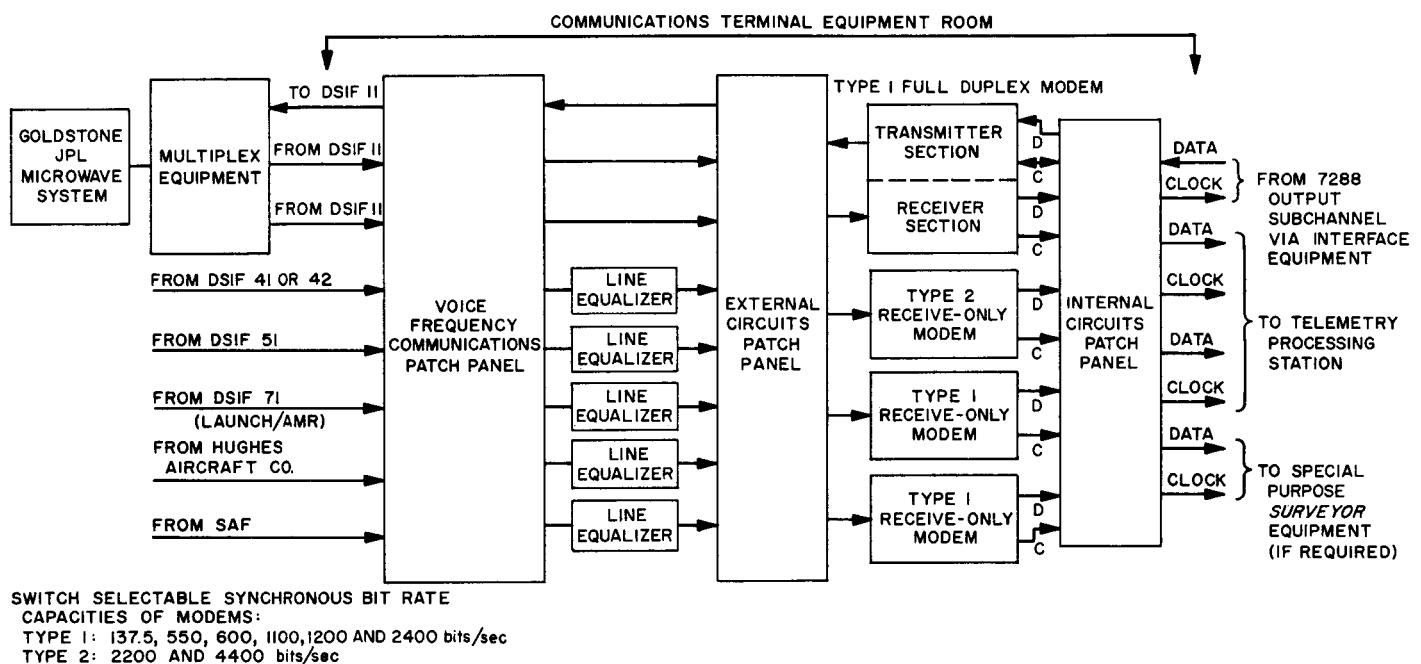

Fig. 3. SFOF high-speed data communications subsystem

SPACE SCIENCES

VIII. Space Instrument Systems

A. Planetary Scan Subsystem (Mariner C)

The planetary scan subsystem, designed and developed at JPL, has been incorporated in the *Mariner C* spacecraft. A functional block diagram of this subsystem is shown in Fig. 1. The purpose of the subsystem is to acquire and track the planet Mars so that the planetary instruments are correctly oriented to perform encounter measurements. The design requirements and detailed operation of the subsystem have been described in Refs. 1 and 2.

Radiation energy experiments. As design data for the subsystem, the amount of solar energy reflected from
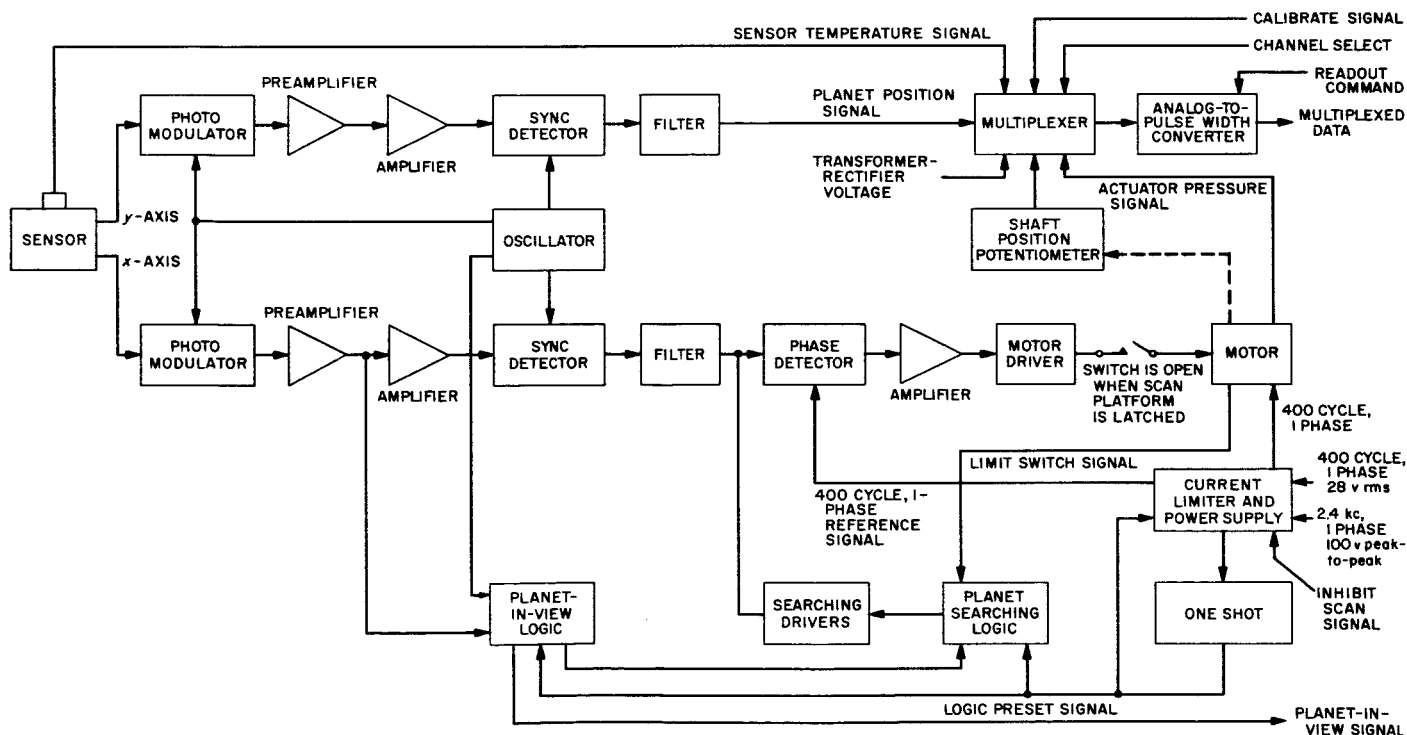
Fig. 1. Scan subsystem

Mars and incident at the sensor was calculated based on theoretical considerations. To verify the validity of the calculated values and to obtain data for the design of future subsystems, experiments will be performed during the encounter to determine the magnitude of the integrated energy incident at the sensor in the spectral range of 0.5 to 1.1 μ.

The radiation sensor is a silicon p-n junction device which converts the x-y coordinates of the planet image on its surface into a pair of voltages V_x and V_y. The magnitude of these signals is a function of the planet position, fly-by distance and the amount of radiant energy received. The x-axis output is utilized as the error signal for planet tracking while the y-axis output determines the angular position of the planet with respect to the sensor and the amount of radiant energy received. Fig. 2 shows curves of the y-axis output as a function of the simulated planet angular position with the calculated

radiant energy as the parameter. The curves were generated by holding the simulated planet-to-sensor distance constant. It is seen from these curves that by holding the fly-by distance fixed, the magnitude of the y-axis output is a function of the planet angular position as well as the amount of radiant energy received. Similar sets of curves can be generated at various simulated fly-by distances as calibration data. A number of sets of these calibration curves are required to interpret the flight data since the y-axis output is a function of the planet-to-sensor distance as well as the planet angular position in an actual flight trajectory.

It is well known that the power sensitivity of the silicon sensor is a function of the operating temperature. This temperature-dependence problem can be compensated for either by deriving equations relating power sensitivity to the operating temperature or by generating additional sets of calibration curves at various temperatures.

Additional information can be derived from these curves. As the planet image approaches along the x-axis and becomes centered on the origin, the y-axis output decreases to a value equal to the output value with zero energy input and then decreases further as the image passes beyond the origin along the −x-axis. The slope of the curves at the point of zero energy input is a function of the planet angular diameter. Since the planet angular diameter is directly related to the planet-to-sensor distance by the known geometry of the optical system, the approximate fly-by distance can be calculated from the observed numerical value of the slope.

Subsystem packaging. The subsystem was fabricated and packaged in three units as shown on Fig. 3: 31A1—preamplifier, optics and sensor assembly; 31A2—power supply and electronics; and 31A3—electronics.

Unit 31A1, designed and packaged for mounting on the scan platform, consists of a lens barrel with optics, sensor housing with the sensor, preamplifier circuits, and photomodulators. All electronic components of this unit are mounted on a subchassis as shown on Fig. 4 (preamplifier cover removed). The remaining electronic components of the subsystem are mounted on two *Mariner C* basic subchassis to form Units 31A2 and 31A3. These two units are to be located in Electronics Assembly III for scientific equipment in the octagonal instrument compartment.
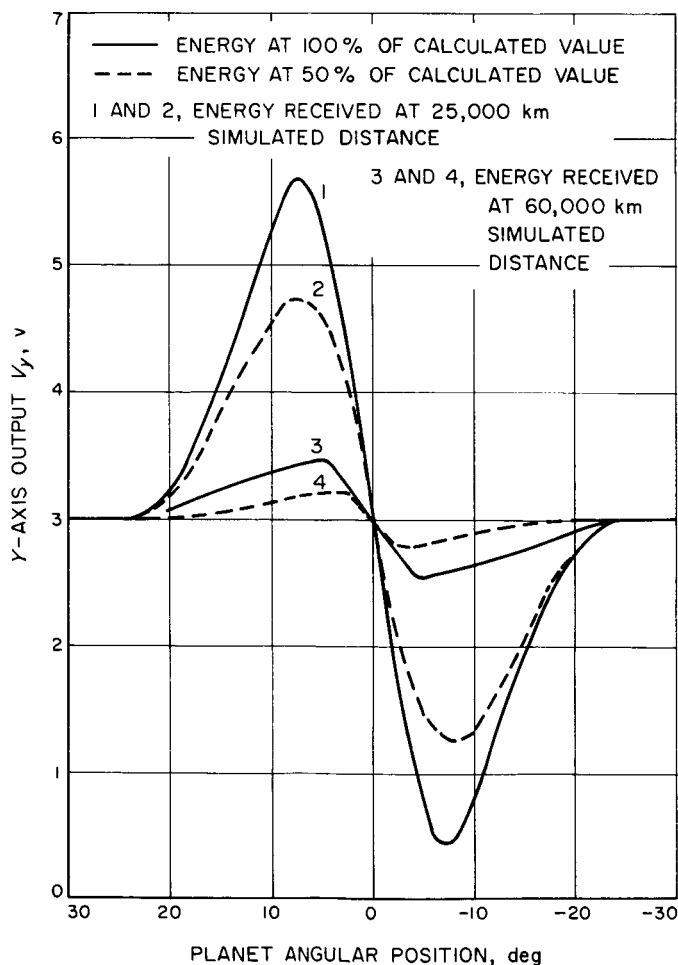

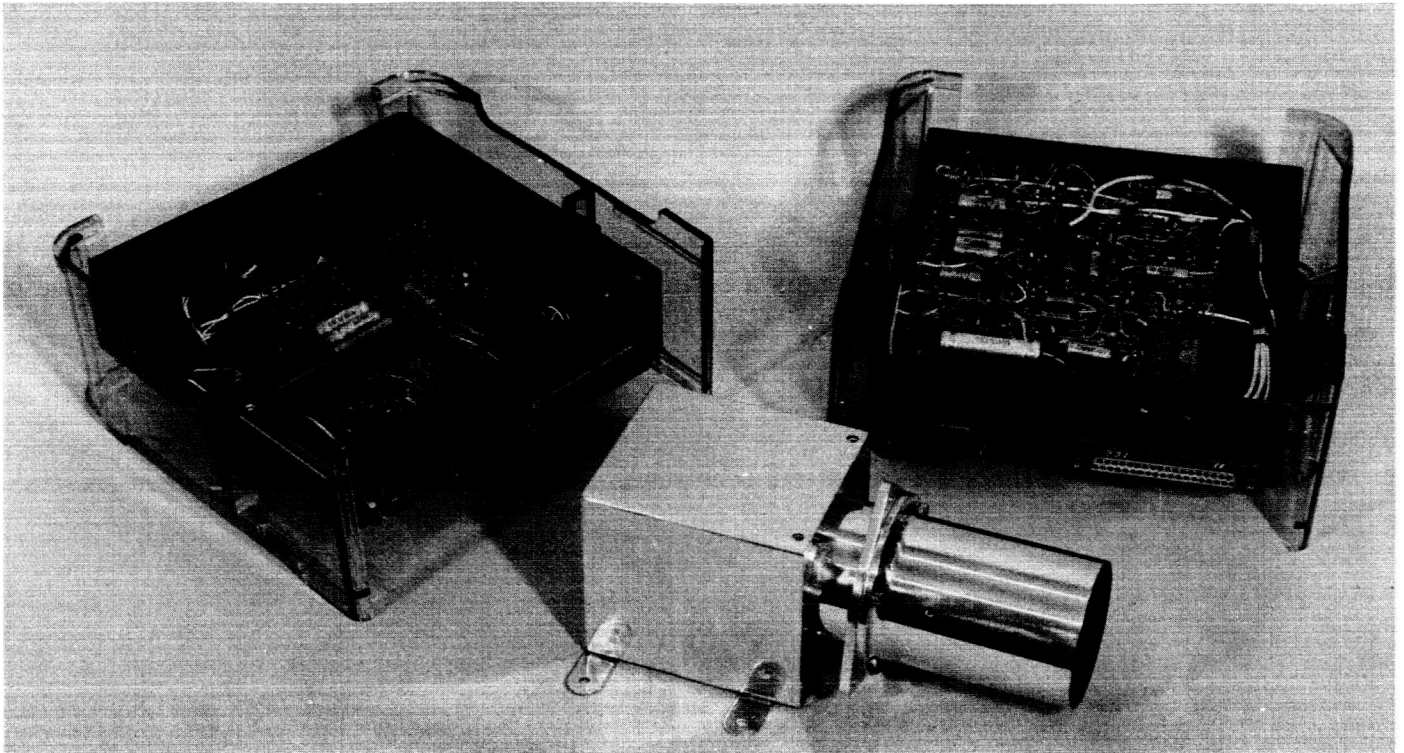**Fig. 2. y-axis output as a function of planet position**
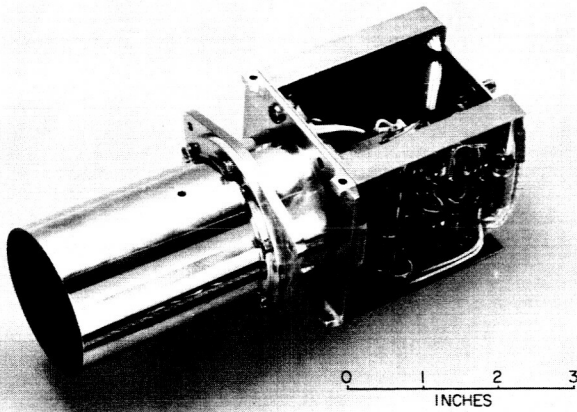
Fig. 3. Subsystem packaging

Fig. 4. Preamplifier, optical and sensor assembly

Fig. 5. Planetary scan logic modules

To conserve weight, volume, and power consumption without sacrificing reliability, thin-film microcircuit networks manufactured by Texas Instruments, Inc., were utilized in the searching, tracking, and planet-in-view logic circuits. These semiconductor networks, along with the other logic electronic components, are packaged in welded modules in order to take advantage of their physical configuration and small dimensions. Fig. 5

shows the two modules containing these logic circuits. Module 1, having dimensions of 1.20 × 0.57 × 0.40 in., contains 5 flip-flops, 2 *nor* gates, 2 resistors, and 2 capacitors. Module 2, with dimensions of 1.50 × 0.47 × 0.43

in., consists of 4 flip-flops, 4 *nor* gates, 5 diodes, and 3 resistors.

Subsystem type-approval testing. Type-approval environmental tests were performed to verify the subsystem's capabilities and performance under simulated flight environments. Upon completion of the mechanical testing, all units were carefully inspected for possible mechanical damage. The thermal–vacuum tests were divided into a number of test cycles, each consisting of a complete operational sequence.

Test results indicated that the subsystem has successfully passed all tests and the performance was within the limits specified by the design requirements. Bench checkout upon completion of the type-approval tests indicated that there was no apparent degradation in performance.

References

1. "Planetary Scan System," *SPS 37-18*, Vol. VI, pp. 70–72, Jet Propulsion Laboratory, Pasadena, California, December 31, 1962.

2. "Planetary Scan Subsystem for *Mariner* Mars 1964," *SPS 37-21*, Vol. VI, pp. 75–78, Jet Propulsion Laboratory, Pasadena, California, June 30, 1963.

IX. Applied Science

A. *Surveyor* Single-Axis Short-Period Seismometer

The *Surveyor* single-axis short-period seismometer sensor with lunar springs, available since mid-1962, has been tested for period and damping characteristics (Ref. 1). An auxiliary spring fixture, compensating for ⅚ of the mass weight, was used for these tests. During November 1963, the sensor was refitted with Earth springs and was mated with an engineering prototype amplifier and power supply. The seismometer sensor is shown in Fig. 1 with a microscope used to center the seismic mass. The amplifier and power supply electronics breadboard unit is shown in Fig. 2. The springs which were used produced a natural frequency of the seismic mass of 1.22 cps. The electromagnetic damping is set near critical. This then produces, in the Earth's gravitational field, conditions similar to those in which the lunar seismometer will operate.
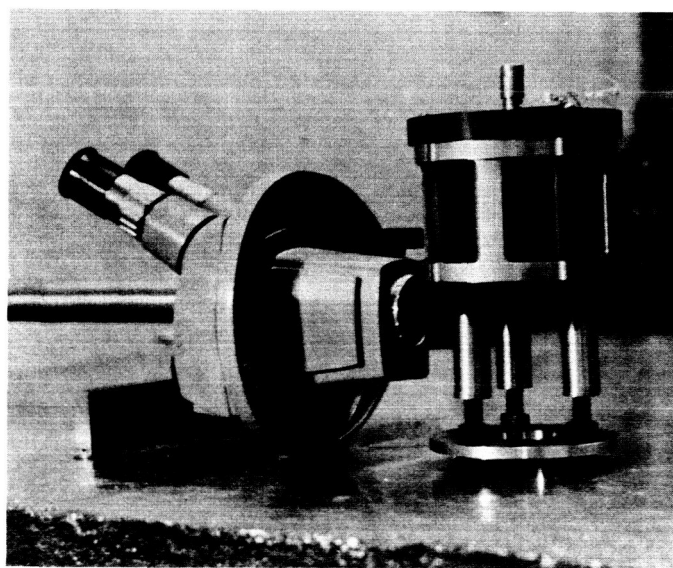

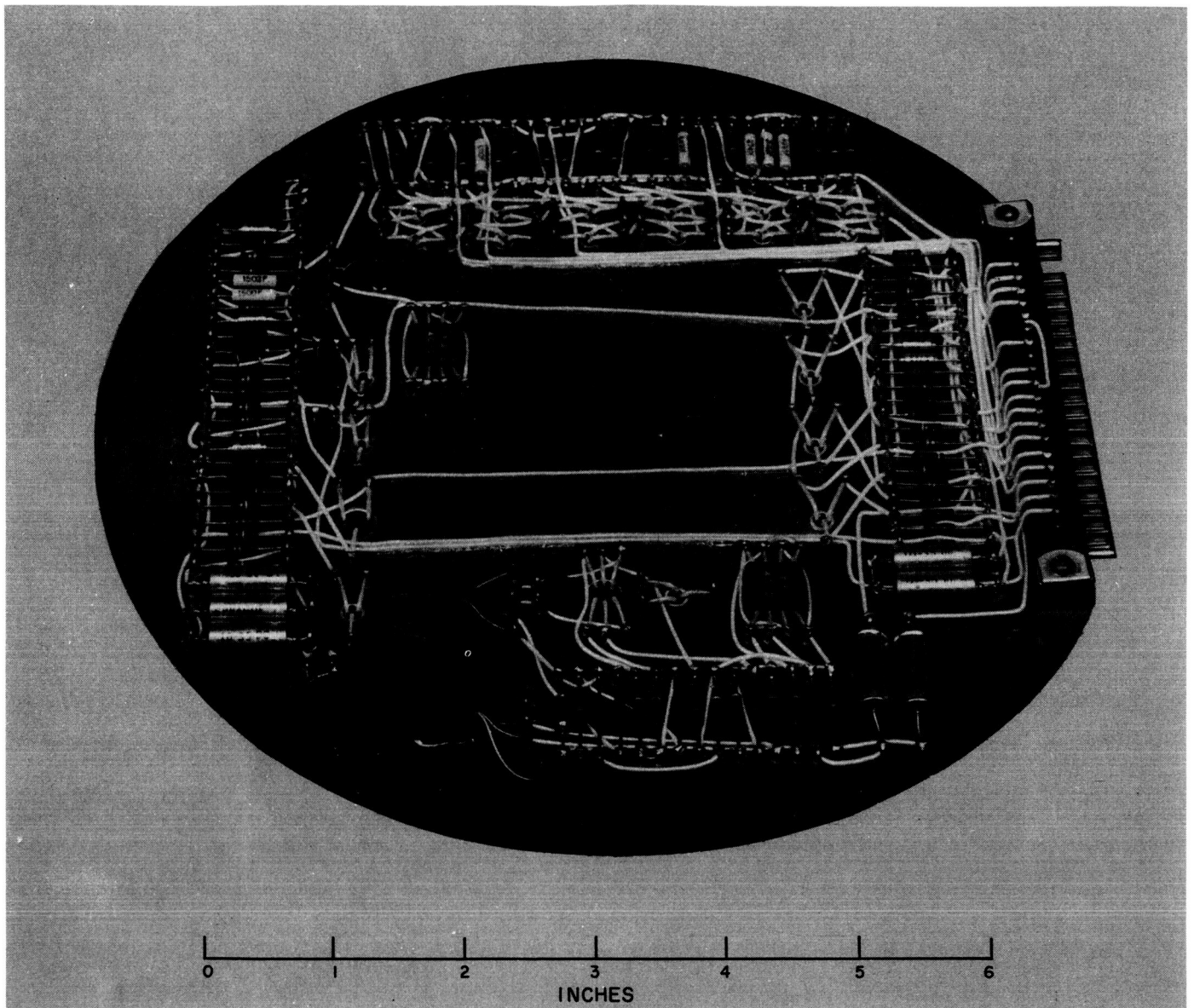Fig. 1. *Surveyor* single-axis short-period seismometer with centering microscope

Fig. 2. Seismometer amplifier and power supply electronics breadboard unit

The sensor was placed on the Lamont Geological Observatory seismic pier at Palisades, New York, and the output was recorded on a helical drum recorder (Fig. 3) with a drum speed of 4 rph. On the deployed recording (Fig. 4), successive traces correspond to a 15-min time interval. Intervals of 1 min are indicated by the time marks on the recording. Time notations refer to eastern standard time.

Two events recorded on December 17, 1963, at 7:48:40 and 7:59:20 p.m. correspond to the arrival of a PKP wave

(i.e., a compression wave that travelled partially through the Earth's core). The quakes originated in the Tonga Island region (South Pacific, 173-deg west longitude, 20-deg south latitude). The first quake, the larger of the two, had a magnitude of 7¼ to 7½; the second had an indefinite magnitude. The travel time from Tonga to Palisades was 18.5 min. This represents an arc of 115.5 deg (111.2 km/deg), or an arc length of 12,850 km (7980 miles).

The December 18, 1963, record shows progressive buildup of the microseism level (storm). Two prominent
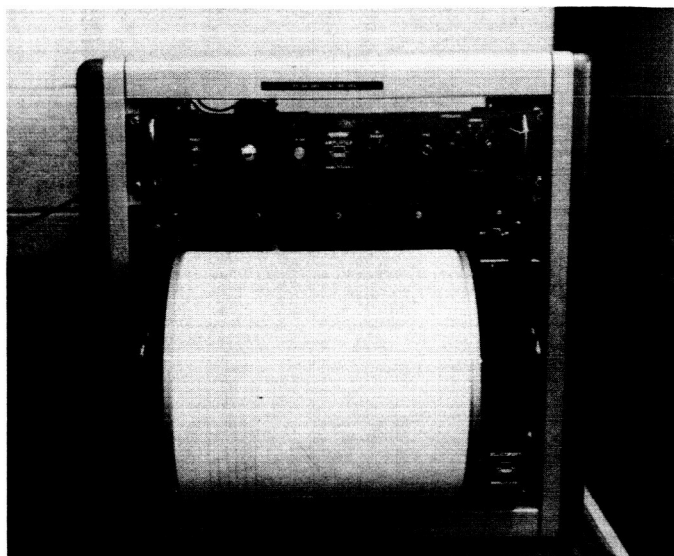
Fig. 3. Helical drum recorder

disturbances at 2:12:30 and 4:56:30 p.m. are believed to have been caused by quarry blasts some 100 km (60 miles) away. The short duration of the disturbances and the high frequencies are two characteristics that help to distinguish these from quakes. Other short-duration high-frequency perturbations were traced to someone walking or working near the pier.

Other tests were made with the breadboard unit to establish the ultimate sensitivity of the sensor. A 0.1-mμ (1 A) displacement at 1 cps was found to correspond to a signal-to-noise ratio of 1. A 1-mμ displacement will yield a signal that is easily detected.

Tests will be conducted in the near future with a prototype sensor (Fig. 5) and electronics. The design improvements incorporated in the prototype should result in improvements in over-all sensitivity.
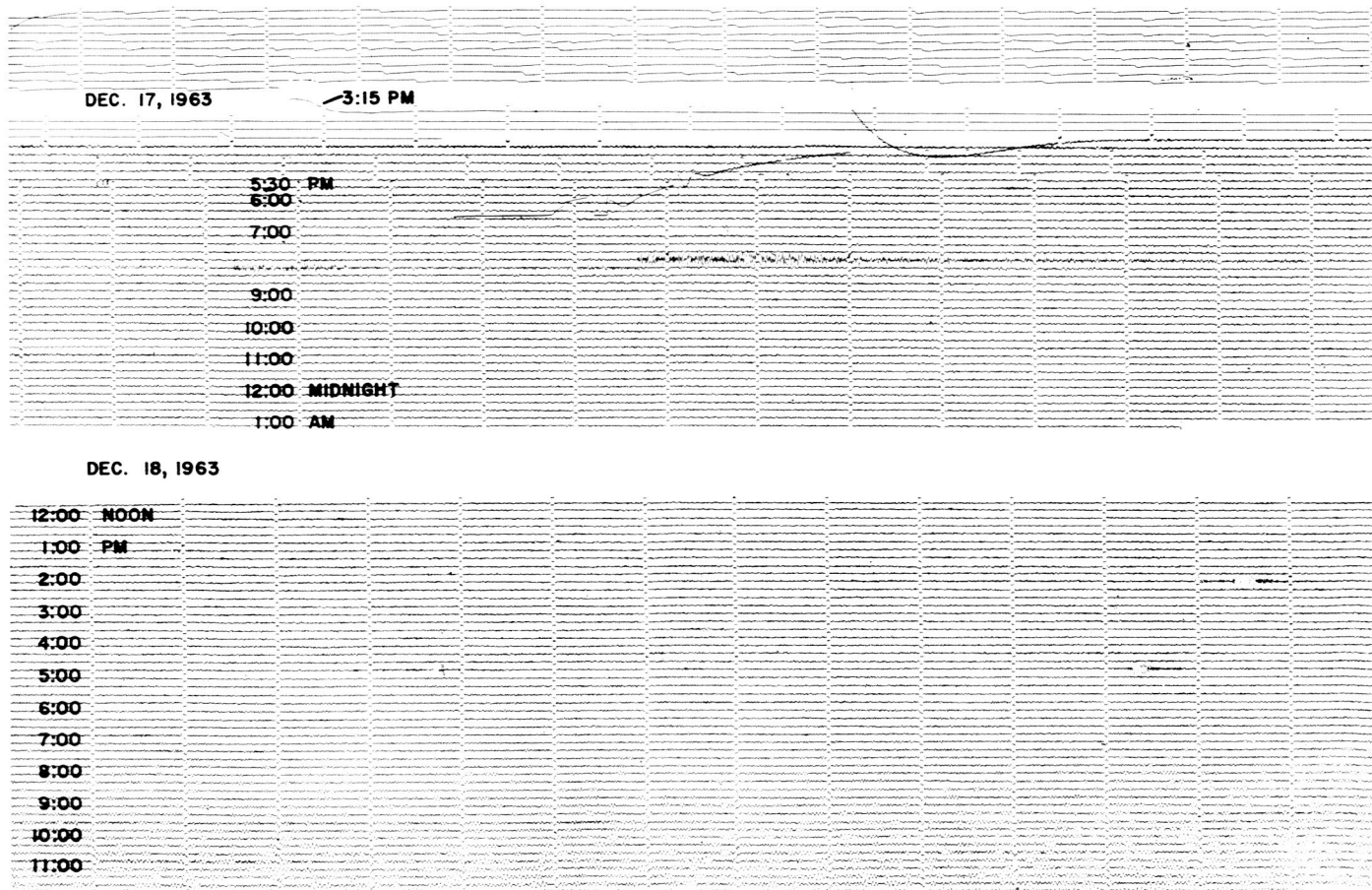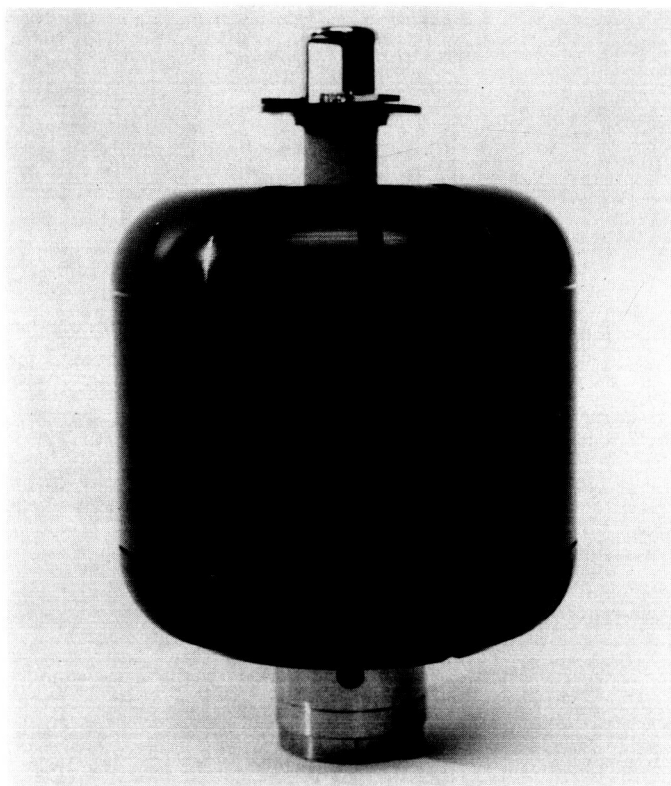

Fig. 4. Seismic recording

**Fig. 5. Prototype single-axis short-period
seismometer sensor**

Reference

1. "Seismograph," *SPS 37-20, Vol. VI,* pp. 90, 91, Jet Propulsion Laboratory, Pasadena, California, April 30, 1963.